Title:

β-adrenergic blockers increase cAMP and stimulate insulin secretion through a PKA/RYR2/TRPM5 pathway in pancreatic β-cells in vitro

Naoya Murao[1,2], Risa Morikawa[1], Yusuke Seino[1,2], Kenju Shimomura[3], Yuko Maejima[3], Yuichiro Yamada[1,2], Atsushi Suzuki[1]

[1] Department of Endocrinology, Diabetes and Metabolism, Fujita Health University, School of Medicine, Toyoake, Japan

[2] Yutaka Seino Distinguished Center for Diabetes Research, Kansai Electric Power Medical Research Institute, Kyoto, Japan

[3] Department of Bioregulation and Pharmacological Medicine, Fukushima Medical University School of Medicine, Fukushima, Japan

Running Title

β-blockers can increase cAMP and insulin secretion in β-cells

Corresponding author, lead contact

Naoya Murao, M.D., Ph.D.

Departments of Endocrinology, Diabetes and Metabolism, Fujita Health University, School of Medicine, 1-98 Dengakugakubo, Toyoake, Aichi 4701192 Japan

Phone: +81-562-93-2699

Fax: +81-562-95-1879

E-mail: muraonaoy@gmail.com

Abbreviations

AC, adenylyl cyclase

BHQ, 2,5-di-*tert*-butylhydroquinone

cAMP, adenosine 3',5'-Cyclic Monophosphate

CICR, Ca^{2+}-induced Ca^{2+} release

ER, endoplasmic reticulum

FKBP, FK-506-binding protein

GPCR, G-protein coupled receptor

GLP-1, glucagon-like peptide

GIP, Glucose-dependent insulinotropic polypeptide

GSIS, glucose-stimulated insulin secretion

iAUC, incremental area under the curve

IP1, inositol 1-phosphate

IP_3, inositol 1,4,5-trisphosphate

K_{ATP} channel, ATP-sensitive K^+ channel

Propranolol-SIS, propranolol-stimulated insulin secretion

PKA, protein kinase A

PKC, protein kinase C

PLCβ, phospholipase Cβ

SERCA, sarcoplasmic/endoplasmic reticulum Ca^{2+} ATPase

TRPM, Transient receptor potential cation channel subfamily M

VDCC, voltage-dependent Ca^{2+} channel

β-blocker-SIS, β-blocker-stimulated insulin secretion

Abstract

β-adrenergic blockers (β-blockers) are extensively utilized in the treatment of various cardiovascular conditions. However, their direct effects on insulin secretion from pancreatic β-cells remain largely unexplored. This study investigates the impact of β-blockers on insulin secretion utilizing MIN6-K8 clonal β-cells and mouse islets in vitro. Various non-selective and β1-selective β-blockers were found to amplify glucose- and glimepiride-induced insulin secretion 1.5–2 fold. Surprisingly, β-blockers (propranolol and bisoprolol) were found to increase cAMP production 5–10 fold via adenylyl cyclase, the effects being dependent on α2-adrenoceptors, which suggests cross-reactivity of these β-blockers and their receptors. Propranolol-stimulated insulin secretion involves a novel signaling pathway mediated by protein kinase A (PKA), ryanodine receptor 2 (RYR2), and transient receptor potential cation channel subfamily M member 5 (TRPM5). Initially, cAMP activates PKA and triggers RYR2 phosphorylation and extracellular Ca^{2+} influx, leading to Ca^{2+}-induced Ca^{2+} release (CICR). Subsequently, CICR activates TRPM5, resulting in augmented extracellular Ca^{2+} influx through the L-type voltage-dependent Ca^{2+} channel (VDCC). Remarkably, propranolol effectively increased cAMP levels and insulin secretion in diabetic NSY.B6-A^y mouse islets, suggesting a potential strategy for restoring cAMP-stimulated insulin secretion in diabetic β-cells. Our findings provide insights into the fundamental pharmacology of adrenoceptors and the regulatory mechanisms of insulin secretion.

Significance statement

β-adrenoceptors transduce intracellular signals by increasing intracellular cAMP production, an effect that is therapeutically blocked by β-adrenergic blockers (β-blockers) in their standard use. This study investigated the effects of high-dose β-blockers on insulin secretion from pancreatic β-cells in vitro. Strikingly, these concentrations of β-blockers were found to paradoxically increase cAMP production, leading to enhanced insulin secretion via a novel signaling pathway mediated by protein kinase A (PKA) and ryanodine receptor 2 (RYR2). Our results clarify an unexpected pharmacological action of β-blockers, which presents a promising strategy for the restoration of insulin secretion in diabetic β-cells.

Introduction

Pancreatic β-cells secrete insulin to maintain blood glucose levels within a physiological range. Glucose metabolism leads to an increase in intracellular ATP levels which inhibits ATP-sensitive K^+ (K_{ATP}) channels, resulting in membrane depolarization and opening of the voltage-dependent Ca^{2+} channels, increasing intracellular Ca^{2+} ($[Ca^{2+}]_i$) levels and thereby stimulating insulin granule exocytosis.

Insulin secretion is also modulated by various nutrients, hormones, and neurotransmitters, including catecholamines (Porte, 1969). Catecholamines act on adrenergic receptors (adrenoceptors), which are G-protein coupled receptors (GPCRs) comprising nine subtypes: α1 (α1A, α1B, α1D), α2 (α2A, α2B, α2C), and β (β1, β2, β3) (Varney and Benovic, 2024).

Catecholamines, specifically noradrenaline and adrenaline, have been demonstrated to inhibit insulin secretion (Schuit and Pipeleers, 1986; Sluga et al., 2022). These effects are attributed to α2-adrenoceptors and the subsequent activation of Gαi/o of trimeric G proteins, including inhibition of adenylyl cyclase (AC)-mediated adenosine 3',5'-Cyclic Monophosphate (cAMP) production (Straub and Sharp, 2012).

Conversely, β-adrenoceptors are primarily coupled to Gαs, which activates AC to increase intracellular cAMP levels (Brodde et al., 2006). Activation of β-adrenoceptors with their agonists (β-agonists) increases circulating insulin levels in mice and humans in vivo (Porte, 1967; Cerasi et al., 1969; Imura et al., 1971; Loubatières et al., 1971; Ahren and Lundquist, 1981). Although the mechanism underlying the insulinotropic properties of β-agonists has not been fully elucidated, it is reasonable to postulate that β-adrenoceptor-mediated cAMP production potentiates insulin exocytosis via PKA and Epac2 (Seino and Shibasaki, 2005; Tengholm and Gylfe, 2017).

β-adrenoceptor antagonists (β-blockers) function primarily by binding to β1-, β2-, or both adrenoceptors and antagonizing the actions of endogenous catecholamines and β-adrenergic

agonists at these receptors (Paul, 2021). This class of drugs is used to treat various diseases, including tachycardia, hypertension, congestive heart failure, cardiac arrhythmias, hyperthyroidism, essential tremor, glaucoma, migraine prophylaxis, and other conditions (Farzam et al., 2023).

Studies have demonstrated that β2-selective blockers antagonize the insulinotropic effects of exogenous β-adrenergic agonists in vivo (Loubatières et al., 1971; Ahren and Lundquist, 1981), suggesting the involvement of β2-adrenoceptors in insulin secretion. However, the direct effect of β-blockers on insulin secretion has not been sufficiently investigated. This issue is clinically significant because the use of β-blockers is occasionally associated with hypoglycemia (Carnovale et al., 2021).

In the present study, we demonstrate that β-blockers, when administered at high concentrations, paradoxically stimulate cAMP production and insulin secretion in mouse β-cells in vitro. Moreover, characterization of propranolol-SIS reveals a novel insulin secretory pathway involving PKA/RYR2/TRPM5. These findings provide insights into the regulatory mechanism of insulin secretion and the fundamental pharmacology of adrenoceptors.

Materials and Methods

Animals

C57BL/6JJcl (RRID:IMSR_JCL:JCL:MIN-0003) mice were purchased from CLEA Japan (Tokyo, Japan) and used for experiments at 19–20 weeks of age. NSY.B6-*Tyr*+, A^y/Hos mice were a gift from Hoshino Laboratory Animals (Ibaraki, Japan) and were used for experiments at 19–20 weeks of age. Mice were maintained under specific-pathogen-free conditions at 23 ± 2 °C and 55 ± 10% relative humidity with 12-hour light-dark cycles (8am–8pm), with free access to water and standard chow CE-2 (CLEA Japan, Tokyo, Japan). The health status of the mice was checked regularly. All experiments were performed using male mice. Body weight and blood glucose levels were measured at 9am in the ad-lib-fed state. All animal experiments were performed with the approval APU22080 by the Institutional Animal Care and Use Committee of Fujita Health University, complying with the Guidelines for Animal Experimentation at Fujita Health University and current Japanese guidelines and regulations for scientific and ethical animal experimentation (Kagiyama et al., 2006).

Cell lines

MIN6-K8 cells were generated as previously described (Iwasaki et al., 2010) and were kindly provided by Professor Junichi Miyazaki (Osaka University). *Kcnj11*$^{-/-}$ β-cells (clone name: *Kcnj11*$^{-/-}$βCL1) are β-cells deficient in Kir6.2, a pore-forming subunit of the K_{ATP} channel. They were established by sub-cloning MIN6-K8 cells transfected with Cas9 nickase and guide RNA pairs targeting mouse *Kcnj11*, as described previously (Oduori et al., 2020). All cells were cultured in Dulbecco's modified Eagle's medium (DMEM) containing 4500 mg/L glucose (Sigma-Aldrich, St. Louis, MO, USA, Cat# D5796) supplemented with 10% fetal

bovine serum (FBS) (BioWest, Nuaillé, France, Cat# S1400-500) and 5 ppm 2-mercaptoethanol. The cells were maintained at 37 °C with 5% CO_2.

Reagents

2.8 mM glucose-supplemented Krebs-Ringer bicarbonate buffer-HEPES (2.8G-KRBH) was prepared by supplementing KRBH (133.4 mM NaCl, 4.7 mM KCl, 1.2 mM KH_2PO_4, 1.2 mM $MgSO_4$, 2.5 mM $CaCl_2$, 5 mM $NaHCO_3$, 10 mM HEPES, pH 7.4) with 0.1% bovine-serum albumin (Sigma-Aldrich, St. Louis, MO, USA, Cat# A6003) and 2.8 mM glucose. Ca^{2+}-free KRBH was formulated by replacing $CaCl_2$ with an equimolar $MgCl_2$ and adding 0.2 mM EGTA (NACALAI TESQUE, Kyoto, Japan, Cat# 15214-21). For extracellular Na^+ depletion experiments, control buffer (150 mM NaCl, 5 mM KCl, 1.2 mM KH_2PO_4, 1 mM $MgCl_2$, 2.2 mM $CaCl_2$, 10 mM HEPES, pH 7.4) and Na^+-free buffer [150 mM N-Methyl-D-glucamine (Tokyo Chemical Industry, Tokyo, Japan, CAS: 6284-40-8, Cat# M0227), 5 mM KCl, 1.2 mM KH_2PO_4, 1 mM $MgCl_2$, 2.2 mM $CaCl_2$, 10 mM HEPES, pH 7.4] were prepared. 30 mM Na^+ buffer was formulated by mixing the control buffer and Na^+-free buffer at a ratio of 1:4 and supplementing 0.1% bovine-serum albumin (Sigma-Aldrich, St. Louis, MO, USA, Cat# A6003) and 2.8 mM glucose.

The following reagents were added to KRBH during the stimulation period: 11.1 mM glucose, (±)-propranolol hydrochloride (FUJIFILM Wako Pure Chemical, Osaka, Japan, CAS: 318-98-9, Cat# 168-28071), carteolol hydrochloride (Tokyo Chemical Industry, Tokyo, Japan, CAS: 51781-21-6, Cat# C3015), nadolol (Sigma-Aldrich, St. Louis, MO, USA, CAS: 42200-33-9, Cat# N1892), timolol maleate (Tokyo Chemical Industry, Tokyo, Japan, CAS: 26921-17-5, Cat# T2905), bisoprolol hemifumarate (Tokyo Chemical Industry, Tokyo, Japan, CAS: 104344-23-2, Cat# B3994), metoprolol tartrate (Tokyo Chemical Industry, Tokyo, Japan, CAS: 56392-17-7, Cat# M2555), glimepiride (Tokyo Chemical Industry, Tokyo, Japan, CAS:

93479-97-1, Cat# G0395), and carbamylcholine chloride (carcachol) (Tokyo Chemical Industry, Tokyo, Japan, CAS: 51-83-2, Cat# C0596).

The following reagents were added to KRBH during the pre-incubation and stimulation periods: nifedipine (FUJIFILM Wako Pure Chemical, Osaka, Japan, Cat# 14505781), thapsigargin (FUJIFILM Wako Pure Chemical, Osaka, Japan, CAS: 67526-95-8, Cat# 209-17281), MDL-12330A hydrochloride (Sigma-Aldrich, St. Louis, MO, USA, CAS: 40297-09-4, Cat# M184), SQ22536 (Selleck Chemicals, Houston, TX, USA, CAS: 17318-31-9, Cat# S8283), H-89 hydrochloride (Cayman Chemical, Ann Arbor, MI, USA, CAS: 130964-39-5, Cat# 10010556), phentolamine mesylate (Tokyo Chemical Industry, Tokyo, Japan, CAS: 65-28-1, Cat# P1985), atipamezole hydrochloride (FUJIFILM Wako Pure Chemical, Osaka, Japan, CAS: 104075-48-1, Cat# 015-25331), dantrolene sodium salt hydrate (Tokyo Chemical Industry, Tokyo, Japan, CAS: 14663-23-1, Cat# D3996), triphenylphosphine oxide (Tokyo Chemical Industry, Tokyo, Japan, CAS: 791-28-6, Cat# T0625), YM-254890 (FUJIFILM Wako Pure Chemical, Osaka, Japan, CAS: 568580-02-9, Cat# 257-00631), t-butylhydroquinone (Tokyo Chemical Industry, Tokyo, Japan, CAS: 1948-33-0, Cat# 027-07212), and xestospongin C (FUJIFILM Wako Pure Chemical, Osaka, Japan, CAS: 244-00721, Cat# C0598). The reagents used for stimulation were stored as a 1000× concentrate in dimethyl sulfoxide (DMSO) (FUJIFILM Wako Pure Chemical, Osaka, Japan, Cat# 041-29351) and diluted with KRBH shortly before the experiment. An equal volume of DMSO was added to the vehicle control.

Isolation of pancreatic islets from mice

Digesting solution was formulated by supplementing 0.1w/v% Collagenase from Clostridium histolyticum (Sigma-Aldrich, St. Louis, MO, USA, Cat# C6885) to Hanks' balanced salt solution (136.9 mM NaCl, 5.4 mM KCl, 0.8 mM $MgSO_4$, 0.3 mM Na_2HPO_4, 0.4 mM KH_2PO_4,

4.2 mM $NaHCO_3$, 10 mM HEPES, 1.3 mM $CaCl_2$, 2 mM glucose). The mice were euthanized by isoflurane exposure. Pancreas was digested by 10-min incubation at 37 °C following intraductal injection of digesting solution. Islets were hand-picked and separated from exocrine tissues, transferred to 60-mm non-treated plates (AGC Techno Glass, Shizuoka, Japan, Cat# 1010-060), and cultured overnight in RPMI-1640 (Sigma-Aldrich, St. Louis, MO, USA, Cat# R8758) supplemented with 10% FBS (BioWest, Nuaillé, France, Cat# S1400-500) and 1% penicillin-streptomycin solution (FUJIFILM Wako Pure Chemical, Osaka, Japan, Cat# 168-23191) at 37 °C and 5% CO_2 before the experiments.

Insulin secretion and content

Insulin secretion was measured using the static incubation method, as described previously (Murao et al., 2022; Murao et al., 2024b). To measure insulin secretion from cell lines, the cells were seeded in 24-well plates (Corning, Glendale, AZ, USA, Cat# 353047) at a density of 5×10^5 cells/well and cultured for 48 h. The cells were pre-incubated for 30 min with 300 μL/well of 2.8G-KRBH and subsequently stimulated with 300 μL/well of 2.8G-KRBH containing the specified stimulations for 30 min at 37 °C. The supernatant was collected for the measurement of secreted insulin, after which the cells were extracted with 0.1% Triton-X in 2.8G-KRBH for the measurement of insulin content. Insulin was quantified using a homogeneous time-resolved fluorescence assay (HTRF) Insulin Ultrasensitive kit (Revvity, Waltham, MA, USA, Cat# 62IN2PEH) in accordance with the manufacturer's instructions. To measure insulin secretion from islets, overnight cultured islets were rinsed twice with 2.8G-KRBH, followed by pre-incubation with 2.8G-KRBH for 30 min at 37 °C. Size-matched islets were hand-picked and dispensed in a 96-well plate (Corning, Glendale, AZ, USA, Cat# 353072) at 5 islets/well. KRBH (100 μL/well) containing the specified stimulations was added and incubated for 30 min at 37 °C. The supernatant was subjected to insulin quantification as described above.

Measurement of inositol 1-phosphate (IP1)

Intracellular inositol 1-phosphate content was measured as described previously (Murao et al., 2024a). Briefly, MIN6-K8 cells were seeded in a 96-well plate (Corning, Glendale, AZ, USA, Cat# 353072) at a density of 1.0×10^5 cells/well and cultured for 48h. The measurement was performed using IP1 assay buffer (146 mM NaCl, 4.2 mM KCl, 50 mM LiCl, 1 mM CaCl2, 0.5 mM MgCl2, 10 mM HEPES, 0.1% BSA, pH7.4) supplemented with 2.8 mM glucose (2.8G-IP1 assay buffer). The cells were pre-incubated for 30 min with 30 μL/well of 2.8G-IP1 assay buffer, followed by the addition of 10 μL/well of IP1 assay buffer containing the specified stimulations at 4× concentration, and incubation for another 30 min at 37 °C. The reaction was terminated by the addition of 10 μL/well lysis buffer. The lysate (30 μL/well) was transferred to a 384-well plate (Cat #3826; Corning, Glendale, AZ, USA) and subjected to IP1 quantification using the HTRF IP-One Gq Detection Kit (Revvity, Waltham, MA, USA, Cat# 62IPAPEB), according to the manufacturer's instructions.

Measurement of cAMP

To prevent cAMP hydrolysis, 2.8G-KRBH was supplemented with 100 μM isobutylmethylxanthine (IBMX) for pre-incubation and stimulation. To measure cAMP levels in MIN6-K8 cells, the cells were seeded in a 96-well plate (Corning, Glendale, AZ, USA, Cat# 353072) at a density of 1.0×10^5 cells/well and cultured for 48h. The cells were pre-incubated for 30 min with 40 μL/well of 2.8G-KRBH, followed by the addition of 20 μL/well of 2.8G-KRBH containing the specified stimulations at 4× concentration, and incubation for another 30 min at 37 °C. The reaction was terminated by the addition of 20 μL/well lysis buffer. The lysate (20 μL/well) was transferred to a 384-well plate (Cat #3826; Corning, Glendale, AZ, USA) and subjected to cAMP quantification using the HTRF cAMP Gs Dynamic Detection

Kit (Revvity, Waltham, MA, USA, Cat# 62AM4PEB), according to the manufacturer's instructions.

To measure cAMP levels in islets, overnight cultured islets were rinsed twice with 2.8G-KRBH. Size-matched islets were hand-picked and dispensed in a 96-well plate (Corning, Glendale, AZ, USA, Cat# 353072) at 5 islets/well, followed by pre-incubation with 30 μL/well of 2.8G-KRBH for 30 min at 37 °C. Subsequently, 10 μL/well of 2.8G-KRBH containing the specified stimulations at 4× concentration was added to the wells and incubated for another 30 min at 37 °C. The reaction was terminated by the addition of 15 μL/well lysis buffer. The lysate (20 μL/well) was transferred to a 384-well plate and subjected to cAMP quantification, as described above.

Ca^{2+} imaging

Ca^{2+} imaging was performed as previously described (Murao et al., 2024b). Briefly, MIN6-K8 cells were seeded in a 35 mm glass-bottom dish (Matsunami Glass, Osaka, Japan, Cat# D11530H) at a density of 1.28×10^5 cells/dish and cultured for 48 h. Subsequently, the cells were loaded with 1 μM Fluo-4 AM (Dojindo, Kumamoto, Japan, Cat# F312) in 2.8G-KRBH for 20 min at 37 °C in room air. The cells were loaded with 1 mL of fresh 2.8G-KRBH, and basal recordings were performed for 300 s (from time -300 to 0). Following the addition of 1 mL KRBH supplemented with stimulations at a 2× concentration, recordings were resumed for another 600 s (from time 0 to 600). Time-lapse images were obtained using a Zeiss LSM 980 Airyscan2 inverted confocal laser scanning super-resolution microscope equipped with a Plan Apo 40×, 1.4 Oil DICII objective lens (Carl Zeiss Microscopy, Jena, Germany). The cells were excited at 488 nm laser with 0.3% output power, and fluorescence emission was measured at 508-579 nm. The obtained images were analyzed using the ZEN 3.0 imaging software (Carl Zeiss Microscopy, Jena, Germany, RRID:SCR_021725). Cells were randomly chosen for

analysis for each stimulation, and the number of cells analyzed is indicated in the figure legends. The fluorescence intensity of the entire cell body (F) was monitored and normalized to the average fluorescence intensity between -300 and 0 s (F0).

Gene silencing using small interfering RNA (siRNA)

Gene silencing was performed as previously described (Murao et al., 2024b). The following siRNAs were purchased from Dharmacon (Lafayette, CO, USA): *Adra2a* (Cat# M-062217-01-0005), *Adrb1* (Cat# M-043428-01-0005), *Adrb2* (Cat# M-042042-00-0005), *Itpr1* (Cat# M-040933-01-0005), *Trpm4* (Cat# M-056098-01-0005), *Trpm5* (Cat# M-046645-01-0005), and non-targeting siRNA (Cat# D-001206-14-50). Briefly, siRNAs were reverse-transfected using DharmaFECT 2 transfection reagent (Dharmacon, Lafayette, CO, USA, Cat# T-2002-03) according to the manufacturer's instructions. The final concentrations of siRNA and DharmaFECT 2 were 40 nM and 0.4%, respectively. For insulin secretion experiments, cells were seeded in 24-well plates (Corning, Glendale, AZ, USA, Cat# 353047) at 5×10^5 cells/500 μL/well. For immunoblotting, the cells were seeded in 12-well plates (Corning, Glendale, AZ, USA, Cat# 353043) at 1×10^6 cells/mL/well.

Reverse transcription quantitative polymerase chain reaction (RT-qPCR)

RT-PCR was performed as previously described (Murao et al., 2024b). Briefly, cDNA was prepared using CellAmp Direct Lysis and RT set (Takara Bio, Shiga, Japan, Cat# 3737S/A) according to the manufacturer's instructions. Quantitative real-time PCR was performed on a QuantStudio 7 Flex system (Thermo Fisher Scientific, Waltham, MA, USA, RRID:SCR_020245) using TaqMan Universal Master Mix II with UNG (Thermo Fisher Scientific, Waltham, MA, USA, Cat# 4440038) and Taqman probes as follows: *Adra2a* (Cat# Mm07295458_s1), *Adrb1* (Cat# Mm00431701_s1), *Adrb2* (Cat# Mm02524224_s1), *Itpr1*

(Cat# Mm00439907_m1), *Trpm4* (Cat# Mm00613173_m1), *Trpm5* (Cat# Mm01129032_m1), and TATA-box binding protein (*Tbp*, Cat# Mm01277042_m1). Relative gene expression was calculated using the $2^{-\Delta\Delta CT}$ method and normalized to *Tbp*.

Immunoblotting

Immunoblotting was performed as previously described (Murao et al., 2024b), with slight modifications. Briefly, the cells were lysed with 50 μL/well of RIPA buffer (50 mM Tris-HCl pH 7.4, 150 mM NaCl, 1% NP-40, 0.25% sodium deoxycholate, 1% SDS), supplemented with complete protease inhibitor cocktail (Sigma-Aldrich, St. Louis, MO, USA, Cat# 11697498001) and PhosSTOP (Roche, Basel, Switzerland, Cat# 4906845001). For the detection of ADRA2A, the lysate was separated on a 7.5% polyacrylamide-SDS gel and transferred to a PVDF membrane. The membranes were probed with polyclonal anti-ADRA2A rabbit antibody (Thermo Fisher Scientific, Waltham, MA, USA, Cat# PA1-048, RRID:AB_2225243) overnight at 4 °C. To detect RYR2 phosphorylation, the lysate was separated on a 5% polyacrylamide-SDS gel and transferred to a PVDF membrane. The membranes were probed with either an anti-RYR2 rabbit monoclonal antibody (Abcam, Cambridge, UK, Cat# EPR26288-70, 1:300) or an anti-phospho RyR2 (Ser2808) rabbit polyclonal antibody (Millipore, Burlington, MA, USA, Cat# ABS2231, 1:300) overnight at 4 °C. The membrane was then incubated with HRP-conjugated polyclonal swine anti-rabbit antibody (Agilent Technologies, Santa Clara, CA, USA, Cat# P0399, RRID:AB_2617141, 1:2000) for 1 h at room temperature. Signals were visualized using ECL Prime detection reagent (Cytiva, Buckinghamshire, UK, Cat# RPN2232). To visualize the whole protein in *Adra2a* knockdown samples, the membrane was stained with Ponceau-S solution (Beacle, Kyoto, Japan, Cat# BCL-PSS-01) after immunoblotting. Images were taken using ImageQuant 800 (Cytiva,

Buckinghamshire, UK). The images were quantified using ImageJ (version 1.53k, https://imagej.nih.gov/ij/index.html, RRID:SCR_003070).

Statistical Analysis

Sample sizes were estimated from the expected effect size based on previous experiments. No randomization or blinding was used. For cell line experiments, including insulin secretion, IP1 measurement, cAMP measurement, RT-qPCR, and immunoblotting, n represents the number of biological replicates of cells grown in different wells of the same multiwell plate. Results were confirmed by 2–3 independent experiments performed on different days using different cell passages. For islet experiments, n represents the number of wells, each containing five islets. The number of mice used is indicated in the figure legends. Results were confirmed by two independent experiments performed on different days using different mice. For Ca^{2+} imaging, n represents the number of different single cells analyzed. Data are shown as the mean ± standard deviation (SD) along with the plot of individual data points. For statistical comparisons between two groups, a two-tailed unpaired Welch's unpaired t-test was used. For comparisons between more than three groups, Welch's one-way analysis of variance (ANOVA) was followed by pairwise comparisons corrected using Dunnett's method. Normality of the distribution was confirmed by the Shapiro-Wilk test. P-values are indicated in the figures. P-values less than 0.05 were considered statistically significant. The statistical analyses used are indicated in the figure legends. Statistical analyses were performed using GraphPad Prism 10 (Graphpad Software, Boston, MA, USA, https://www.graphpad.com; RRID:SCR_002798).

Results

β-Blockers amplify insulin secretion from β-cells

The impact of β-blockers on insulin secretion was investigated using MIN6-K8, a mouse clonal β-cell line (Iwasaki et al., 2010), which was stimulated with various non-selective and β1-selective β-blockers at a concentration of 100 μM in the presence of the K_{ATP} channel blocker glimepiride. Surprisingly, all β-blockers tested, with the exception of nadolol, were found to amplify glimepiride-induced insulin secretion by 1.5–2 fold (Figure 1A). In the subsequent experiments, propranolol and bisoprolol were used to explore the characteristics of β-blocker-stimulated insulin secretion (β-blocker-SIS).

In the presence of stimulatory levels (11.1 mM) of glucose, both propranolol and bisoprolol dose-dependently increased insulin secretion at concentrations greater than 10 μM and 100 μM, respectively (Figure 1, B–C). These trends were similarly observed in primary-cultured C57BL/6J (B6) mouse islets stimulated with propranolol in the presence of 11.1 mM glucose (Figure 1, D–E) or glimepiride (Figure 1F). At basal glucose concentration (2.8 mM), propranolol exhibited no effect on insulin secretion (Figure 1G) or insulin content (Figure S1A). To evaluate whether β-blockers enhance insulin secretion by facilitating K_{ATP} channel closure, their efficacy was examined in *Kcnj11*$^{-/-}$ β cells. As *Kcnj11* encodes the pore-forming subunit of the K_{ATP} channel, *Kcnj11*$^{-/-}$ β-cells lack K_{ATP} channel activity, and their cell membrane is continuously depolarized regardless of extracellular glucose levels (Oduori et al., 2020). Propranolol increased insulin secretion in *Kcnj11*$^{-/-}$ β-cells even at 2.8 mM glucose (Figure 1H). These findings suggest that propranolol-stimulated insulin secretion (propranolol-SIS) does not necessitate K_{ATP} channel activity, but does require concurrent membrane depolarization induced by other conditions such as high glucose, sulfonylureas, and *Kcnj11* knockout.

β-Blockers increase cAMP in β-cells

To elucidate the mechanism of β-blocker-SIS, we investigated whether β-blockers modulate canonical GPCR signaling pathways in MIN6-K8 cells.

Propranolol and bisoprolol dose-dependently increased intracellular cAMP levels in MIN6-K8 cells at concentrations that were effective for insulin secretion (Figure 2, A–B). Two adenylyl cyclase (AC) inhibitors, MDL-12330A and SQ-22536, suppressed cAMP accumulation induced by both 100 μM propranolol and 1 mM bisoprolol (Figure 2C, S1B), indicating that β-blocker-induced cAMP accumulation is mediated by the activation of adenylyl cyclase. Furthermore, these inhibitors also abolished propranolol-stimulated insulin secretion (propranolol-SIS) (Figure 2, D–E), indicating that cAMP production via AC is necessary for propranolol-SIS. Notably, propranolol-SIS was also abolished by H-89, a protein kinase A (PKA) inhibitor (Figure 2F), suggesting that the cAMP/PKA pathway is essential for propranolol-SIS.

Next, inositol 1,4,5-trisphosphate (IP_3) production was assessed by the intracellular accumulation of inositol 1-phosphate (IP1), a metabolite of IP_3. IP1 levels remained unaltered by propranolol, although substantial accumulation of IP1 was confirmed using carbachol as a positive control (Figure S1C), indicating that propranolol does not activate the Gαq/PLCβ pathway. This finding is corroborated by the observation that YM-254890, a specific inhibitor of Gαq/11/14 (Takasaki et al., 2004; Patt et al., 2021), suppressed glimepiride-induced insulin secretion (Figure S1D), but minimally affected propranolol-SIS when expressed as a fold-change (Figure S1E). Collectively, these results demonstrate that propranolol-SIS involves the cAMP/PKA pathway, but not the Gαq/PLCβ pathway.

α2-adrenoceptor is involved in propranolol-stimulated cAMP production and insulin secretion

We assessed the involvement of β1- and β2-adrenoceptors, which are pharmacological targets of propranolol, in its insulin secretory effect. Treatment of MIN6-K8 cells with siRNAs targeting *Adrb1* and *Adrb2* only marginally decreased their transcript levels (Figure S2, A–B), with no effect on propranolol-SIS when expressed as fold-change over glimepiride alone (Figure S2, C–F). The low knockdown efficiency may be due to the scarce expression of β-adrenoceptors in MIN6-K8 cells, as indicated by our previously published RNA-seq datasets (Hashim et al., 2018) (Table S1).

The same datasets also revealed a marked prevalence of α2A-adrenoceptors in MIN6-K8 cells and B6 mouse islets (Table S1), necessitating assessment of their involvement in propranolol-SIS. Pretreatment with atipamezole (α2-adrenoceptor antagonist) and phentolamine (α1/2-adrenoceptor antagonist) demonstrated a tendency to increase basal cAMP levels (Figure 3A), presumably confirming their α2-inhibitory effects. Interestingly, both antagonists attenuated propranolol-stimulated cAMP production, as expressed by the fold-change (Figure 3B). These inhibitors also abolished propranolol-SIS (Figure 3, C–D). Although phentolamine elevated glimepiride-induced insulin secretion, presumably owing to its direct inhibitory effect on K_{ATP} channels (Plant and Henquin, 1990; Proks and Ashcroft, 1997), this inhibitor potently suppressed propranolol-SIS (Figure 3D). To further validate the involvement of α2A-adrenoceptors, we conducted siRNA-mediated knockdown of *Adra2a*, which depleted its protein level by 28% (Figure S2, G–H). This knockdown moderately decreased propranolol-SIS, as expressed by the fold change (Figure 3E, S2I). These findings suggest that α2-adrenoceptor activity is required for propranolol-stimulated cAMP production and insulin secretion.

Propranolol potentiates Ca^{2+} response via PKA/RYR2 pathway

We investigated whether propranolol-SIS is triggered by an increase in intracellular Ca^{2+} ($[Ca^{2+}]_i$) using Fluo-4 imaging in MIN6-K8 cells. Propranolol enhanced the glimepiride-induced increase in $[Ca^{2+}]_i$ (Figure 4, A–C). Glimepiride alone elicited oscillatory $[Ca^{2+}]_i$ waves, whereas a combination of glimepiride and propranolol induced a rapid increase in $[Ca^{2+}]_i$, followed by rapid oscillations (Figure 4B).

Notably, propranolol alone elicited a transient $[Ca^{2+}]_i$ increase at 0 min, followed by sporadic spikes (Figure 4, D–E). This propranolol-stimulated Ca^{2+} response was further investigated to elucidate the involvement of extracellular Ca^{2+} and intracellular Ca^{2+} stores. Nifedipine, an inhibitor of L-type voltage-dependent Ca^{2+} channels (VDCC), suppressed the sporadic $[Ca^{2+}]_i$ spikes but not the $[Ca^{2+}]_i$ increase at 0 min indicated by the black arrow (Figure 4F), suggesting that the $[Ca^{2+}]_i$ spikes represent Ca^{2+} influx through L-type VDCCs. In contrast, removal of extracellular Ca^{2+} from the stimulation buffer inhibited both the $[Ca^{2+}]_i$ increase at 0 min and subsequent $[Ca^{2+}]_i$ spikes (Figure 4G). Depletion of intracellular Ca^{2+} stores with 2,5-di-tert-butylhydroquinone (BHQ), an inhibitor of sarcoplasmic/endoplasmic reticulum Ca^{2+} ATPase (SERCA), exerted the same effect (Figure 4H). These results suggest that the initial $[Ca^{2+}]_i$ increase involves both $[Ca^{2+}]_i$ mobilization from the endoplasmic reticulum (ER) and extracellular Ca^{2+} influx and is required for the later VDCC-mediated $[Ca^{2+}]_i$ spikes. Importantly, nifedipine, removal of extracellular Ca^{2+}, and BHQ also abolished propranolol-SIS in the presence of glimepiride (Figure S3, A–C), demonstrating that the propranolol-stimulated Ca^{2+} response is essential for propranolol-SIS.

The mobilization of Ca^{2+} from the ER is mediated by specific ion channels, such as ryanodine receptors (RYRs) and IP_3 receptors (IP_3Rs), which release Ca^{2+} into the cytosol in response to signaling events (Guerrero-Hernández et al., 2019). The involvement of RYRs was investigated using dantrolene, an RYR inhibitor. Dantrolene negated the capacity of propranolol to potentiate the glimepiride-induced Ca^{2+} response in MIN6-K8 cells (Figure 5,

A–B). Dantrolene paradoxically increased glimepiride-induced insulin secretion, consistent with a previous report (Figure S3D) (Pian-Smith et al., 1986); however, it decreased propranolol-IIS, as expressed by the fold change (Figure 5C), suggesting that the propranolol-stimulated Ca^{2+} response and insulin secretion are dependent on RYR. It has been reported that the open probability of RYR2 is increased by intracellular cAMP through PKA-mediated RYR2 phosphorylation at Ser-2808 (Marx et al., 2000; Wehrens et al., 2006). Remarkably, phosphorylation of RYR2 at Ser-2808 was substantially induced by propranolol alone and further enhanced by the addition of glimepiride (Figure 5, D–E). These findings suggest that the propranolol-stimulated Ca^{2+} response is mediated by PKA-induced RYR2 phosphorylation, corroborating the observation that propranolol-SIS is dependent on PKA activity (Figure 2F).

The involvement of IP_3Rs was investigated using xestospongin C, an IP_3R inhibitor (Gafni et al., 1997), and siRNA-mediated knockdown of IP_3 receptor 1 (Itpr1). Xestospongin C marginally decreased propranolol-SIS (Figure S3, E–F). However, depletion of *Itpr1* by approximately 50% at the transcript level did not affect propranolol-SIS, as expressed by the fold-change (Figure S3, G–I). These findings suggest that IP_3 receptors play a limited, if any, role in propranolol-SIS.

Involvement of TRPM5 in propranolol-stimulated Ca^{2+} response

We investigated the mechanism by which PKA-mediated $[Ca^{2+}]_i$ mobilization from the ER leads to VDCC activation. Interestingly, a reduction in extracellular Na^+ from 150 mM to 30 mM suppressed the propranolol-stimulated Ca^{2+} response and insulin secretion in MIN6-K8 cells (Figure 6, A–B), suggesting the involvement of Na^+-permeable channels. Transient receptor potential cation channel subfamily M member 4 (TRPM4) and member 5 (TRPM5) are Ca^{2+}-activated channels that permeate monovalent cations, including Na^+ and K^+. They are gated by $[Ca^{2+}]_i$, most notably Ca^{2+} from the ER (Zhang et al., 2007; Gonzales et al., 2010).

Notably, TRPM5 has been implicated in the augmentation of glucose-induced depolarizing currents in β-cells (Colsoul et al., 2010), suggesting its potential role as a mediator linking $[Ca^{2+}]_i$ mobilization from the ER to depolarization. To elucidate the involvement of TRPM4 and TRPM5, we conducted siRNA-mediated knockdown, which depleted their mRNA levels by approximately 50% (Figure S4, A–B). Knockdown of *Trpm4* and *Trpm5* led to slight and moderate decreases in propranolol-SIS, respectively (Figure 6C, Figure S4C). Furthermore, triphenylphosphine oxide (TPPO), a TRPM5 inhibitor (Palmer et al., 2010), inhibited the later Ca^{2+} spikes and insulin secretion (Figure 6, D–E). These findings suggest that TRPM5 is involved in the later phase of the propranolol-stimulated Ca^{2+} response, contributing to propranolol-SIS.

Propranolol increases cAMP and insulin secretion in diabetic mouse islets

To assess the pathophysiological significance of the β-blocker-activated PKA/RYR2/TRPM5 pathway, we tested propranolol-SIS in a diabetes mouse model. NSY.B6-*Tyr*+, A^y (NSY.B6-A^y) is a spontaneous type 2 diabetes mouse strain recently established by crossing the NSY and B6J- A^y strains, introducing the obesity-related agouti-yellow (A^y) mutation in the agouti (a) gene into a diabetes-prone NSY background (Ohno et al., 2022). A^y heterozygous male mice (NSY.B6-A^y/*a*) exhibited obesity and hyperglycemia; wild-type male mice (NSY.B6-*a*/*a*) served as lean controls (Ohno et al., 2022; Murao et al., 2024b).

Propranolol increased intra-islet cAMP levels in both strains (Figure 7, A–B). A substantial propranolol-SIS was observed in diabetic A^y/*a* islets at 11.1 mM glucose (Figure 7D), although it did not achieve statistical significance in lean *a*/*a* islets (Figure 7C). At 2.8 mM glucose, no propranolol-SIS was observed in either strain (Figure 7, C–D), confirming the glucose dependency of propranolol-SIS (Figure 1G). These findings suggest the therapeutic potential

of the β-blocker-activated PKA/RYR2/TRPM5 pathway in enhancing insulin secretion from diabetic β-cells.

Discussion

In the present study, we observed a paradoxical effect of β-blockers in stimulating cAMP production and insulin secretion in β-cells. Using propranolol as a representative model, we elucidated the signaling cascade of β-blocker-SIS, as illustrated in Figure 8: (1) propranolol stimulates AC-mediated cAMP production via an unidentified mechanism, resulting in PKA activation; (2) PKA induces RYR2 phosphorylation and extracellular Ca^{2+} influx, leading to Ca^{2+}-induced Ca^{2+} release (CICR); and (3) Ca^{2+} released from the ER activates TRPM5, which augments β-cell electrical activity, extracellular Ca^{2+} influx through L-type VDCC, and insulin secretion.

Previous studies have revealed diverse signaling pathways linking the cAMP signaling to insulin secretion (Seino and Shibasaki, 2005; Tengholm and Gylfe, 2017). Our characterization of the propranolol-induced Ca^{2+} response describes a novel pathway in this system involving PKA/RYR2/TRPM5 (Figure 8). Notably, propranolol evoked a Ca^{2+} response in MIN6-K8 cells even under low-glucose conditions, in which cells are electrically silent. The Ca^{2+} response comprised an immediate transient increase at 0 min and subsequent spikes, the latter indicative of Ca^{2+} influx through L-type VDCCs. We demonstrated that the initial increase in $[Ca^{2+}]_i$ involves $[Ca^{2+}]_i$ mobilization through RYR2, which is facilitated by PKA-mediated RYR2 phosphorylation at Ser 2808. Supporting our findings, it has been suggested that RYR2 activation in β-cells requires cAMP-dependent phosphorylation (Islam et al., 1998). However, that report also indicates that cAMP-dependent phosphorylation alone is insufficient to mobilize Ca^{2+} from the ER when cytosolic $[Ca^{2+}]$ is low (Islam et al., 1998; Islam, 2002); instead, it only sensitizes RYR2 to Ca^{2+}-induced Ca^{2+} release (CICR) by releasing the channel from Mg^{2+}-mediated inhibition (Hain et al., 1994) or FKBP12.6 (FK-506-binding protein 12.6) binding (Marx et al., 2000). Thus, it is reasonable to postulate that propranolol-stimulated cAMP triggers both initial Ca^{2+} influx and RYR2 phosphorylation, leading to CICR, reflected

in the transient rise in $[Ca^{2+}]_i$ at 0 min. The mediator of propranolol-stimulated initial Ca^{2+} influx is currently unclear. However, given that it was inhibited by depletion of extracellular Ca^{2+} and Na^+, but not by nifedipine, cAMP-activated nifedipine-insensitive Ca^{2+} channels, such as T-type VDCCs, may be involved (Louiset et al., 2017; Sharma et al., 2023). A similar mechanism has been proposed for glucagon-like peptide 1 (GLP-1)-stimulated insulin secretion: GLP-1-stimulated cAMP production leading to CICR through a dual effect on Ca^{2+} influx and RYR2 sensitization (Holz et al., 1999).

It is noteworthy that the effect of β-blockers on the cAMP/PKA/RYR2 pathway is contrary to what would be expected from previous studies. In cardiac muscles, β-adrenergic stimulation serves as the primary driver of cAMP/PKA-mediated RYR2 hyperphosphorylation, contributing to heart failure and fight-or-flight responses (Shan et al., 2010a; Shan et al., 2010b). This concept was corroborated by the observation that systemic administration of β-blockers reduces RYR2 phosphorylation and normalizes cardiac cell function in heart failure (Doi et al., 2002; Reiken et al., 2003). However, considering the unexpected pharmacological action of the β-blockers observed in this study, caution is advised when using them to investigate the cAMP/PKA/RYR2 pathway.

TRPM5 and/or TRPM4 have been previously implicated in background inward currents that are increased by GLP-1 (Shigeto et al., 2015) and fructose (Kyriazis et al., 2012). TRPM5 functions downstream of Gαq- or gustducin-coupled GPCR signaling cascades, wherein PLCβ activation triggers Ca^{2+} release from the IP_3 receptor and protein kinase C (PKC) activation, both of which facilitate TRPM5 gating (Shigeto et al., 2015). Our findings suggest that TRPM5 can also be activated downstream of the cAMP/PKA signaling cascade, highlighting its versatile role in linking GPCR signaling and membrane depolarization. Notably, a small background inward current, including that of TRPM5, cannot contribute to depolarization unless the β-cell K_{ATP} channels are predominantly closed (Rorsman and Ashcroft, 2018). This

observation is consistent with the finding that propranolol-SIS is dependent on membrane depolarization induced by high glucose, sulfonylureas, and *Kcnj11* knockout.

This study has several limitations. First, the molecular targets of β-blockers in the stimulation of cAMP production remain unclear. α2-adrenoceptors are abundant in β-cells and mediate the inhibitory effects of adrenaline on insulin secretion (Henquin, 2021; Rorsman and Ashcroft, 2018; Lacey et al., 1993). In particular, mouse β-cells almost exclusively express α2A-adrenoceptors (Rorsman and Ashcroft, 2018). We show that β-blocker-stimulated cAMP production requires the activity of α2A-adrenoceptors, which may imply that propranolol functions as an inverse agonist of α2-adrenoceptors, thereby reducing basal Gi activity. While such a specific interaction has not been previously reported, existing research has indicated similar cross-reactivity between β-selective agents and α-adrenoceptors: (1) bucindolol, a β-blocker, acts as a weak α1-adrenoceptor antagonist (Watts et al., 2000), and (2) isoproterenol, a β-selective agonist, acts as a biased α1A-adrenoceptor agonist (Copik et al., 2014). Experiments using α2A-adrenoceptor knockout mouse β-cell models are necessary to validate this hypothesis. Although the involvement of β-adrenoceptors in β-blocker-SIS cannot be precluded because of their inadequate knockdown efficiency, it is less likely considering their very low expression in MIN6-K8 cells and mouse β-cells (Rorsman and Ashcroft, 2018). However, in human β-cells, β2-adrenoceptors are modestly expressed and mediate transient stimulation of insulin secretion by adrenaline, which is inhibited by propranolol (Henquin, 2021; Lacey et al., 1993). As the presence of β2-adrenoceptors may modify the effect of β-blockers in human β-cells, β-blocker-SIS should also be examined in human islets.

Second, although the present study demonstrates a robust insulinotropic effect of β-blockers in vitro, these effects cannot be extrapolated to in vivo conditions insofar as β-blockers at high concentrations beyond the therapeutic range were used. Specifically, we show that the propranolol concentration must exceed 10 μM to increase insulin secretion from MIN6-K8

cells and mouse islets; the maximum plasma concentration (Cmax) of propranolol in healthy humans is typically less than 1 μM after a single oral dose, as determined by pharmacokinetic analyses (Abdu-Aguye et al., 1986; Taegtmeyer et al., 2014; Kim et al., 2022). Furthermore, its therapeutic range is typically defined as 192 to 385 nM (0.05 to 0.10 μg/mL) with toxicity and mortality range as greater than 7 μM (2 μg/mL) and 11 μM (3 μg/mL), respectively (Kerns, 2007; Sharifpour et al., 2022). Similarly, bisoprolol must be present at concentrations exceeding 100 μM to potentiate insulin secretion, whereas its Cmax should be ≤ 100 nM in vivo (Li et al., 2012; Tjandrawinata et al., 2012).

These discrepancies between in vitro and in vivo β-blocker concentrations present challenges in directly repositioning β-blockers as insulinotropic agents in patients or attributing β-blocker-induced hypoglycemia to their insulinotropic properties. The observations that propranolol did not affect plasma insulin levels when administered to healthy mice (Fagerholm et al., 2008), that nadolol was most significantly associated with hypoglycemia among β-blockers (Carvonale et al., 2021), and that nadolol failed to increase insulin secretion in vitro further underscore the disparity between β-blocker effects in vitro and in vivo.

Nevertheless, β-blocker-stimulated cAMP production remains a noteworthy phenomenon from a therapeutic perspective, as it demonstrates particular efficacy in diabetic NSY.B6-A^y/a mouse β-cells. The current approach to enhance β-cell cAMP signaling relies on incretin-related drugs, such as GLP-1 receptor agonists, dual glucose-dependent insulinotropic polypeptide (GIP) receptor and GLP-1 receptor agonists, and dipeptidyl peptidase-4 (DPP-4) inhibitors. However, these approaches exhibit reduced efficacy in diabetic states compared with healthy conditions. Research has demonstrated that the insulinotropic response to exogenous GIP is diminished in type-2 diabetes (Nauck and Müller, 2023). Although the response to exogenous GLP-1 is relatively preserved in type-2 diabetes (Nauck and Müller, 2023), presumably because of the Gαq/PLCβ pathway, GLP-1-induced cAMP production has

also been suggested to be impaired under hyperglycemic conditions (Oduori et al., 2020). Therefore, our demonstration of β-blocker-stimulated cAMP production in vitro may provide clues to the identification of a novel pathway for the restoration of cAMP signaling and insulin secretion in diabetic β-cells.

Acknowledgements

The authors extend their gratitude to President Yutaka Seino of Kansai Electric Power Hospital for his general support in this research. The authors thank Yoshikazu Hoshino of Hoshino Laboratory Animals, Inc. for providing NSY.B6-A^y mice. The authors thank Shihomi Sakai, Asami Yamaguchi, and Megumi Akiyama for their excellent technical assistance.

Authorship Contributions

Conceptualization, N.M.; Methodology, N.M..; Investigation, N.M., R.M., K.S., and Y.M.; Writing – Original Draft: N.M. and R.M.; Writing – Review & Editing: N.M., R.M., K.S., Y.M., Y.S., Y.Y., and A.S.; Data Curation: N.M. and R.M.; Visualization: N.M. and R.M.; Supervision: K.S., Y.S., Y.Y., and A.S.; Funding Acquisition: N.M. and A.S.

Footnotes

This study was supported by JSPS KAKENHI Grant Numbers JP22K20869 and JP23K15401 for N.M. Research grants for N.M. were provided by the Japan Association for Diabetes Education and Care, Daiwa Securities Foundation, Suzuken Memorial Foundation, Japan Diabetes Foundation, The Hori Sciences and Arts Foundation, Manpei Suzuki Diabetes Foundation, and Fujita Academy.

Conflict of Interest Statement

No author has any actual or perceived conflicts of interest with the contents of this article.

References

Abdu-Aguye I, Dunlop D, Patel P and Turner P (1986) Propranolol pharmacokinetics during the menstrual cycle. Postgraduate Medical Journal 62(734): 1093-1095.

Ahrén B and Lundquist I (1981) Effects of selective and non-selective β-adrenergic agents on insulin secretion in vivo. European journal of pharmacology 71(1): 93-104.

Brodde O-E, Bruck H and Leineweber K (2006) Cardiac adrenoceptors: physiological and pathophysiological relevance. Journal of pharmacological sciences 100(5): 323-337.

Carnovale C, Gringeri M, Battini V, Mosini G, Invernizzi E, Mazhar F, Bergamaschi F, Fumagalli M, Zuccotti G and Clementi E (2021) Beta-blocker-associated hypoglycaemia: New insights from a real-world pharmacovigilance study. British Journal of Clinical Pharmacology 87(8): 3320-3331.

Cerasi E, Effendic S and Luft R (1969) Role of adrenergic receptors in glucose-induced insulin secretion in man. The Lancet 294(7615): 301-302.

Colsoul B, Schraenen A, Lemaire K, Quintens R, Van Lommel L, Segal A, Owsianik G, Talavera K, Voets T and Margolskee RF (2010) Loss of high-frequency glucose-induced Ca^{2+} oscillations in pancreatic islets correlates with impaired glucose tolerance in Trpm5−/− mice. Proceedings of the National Academy of Sciences 107(11): 5208-5213.

Copik AJ, Baldys A, Nguyen K, Sahdeo S, Ho H, Kosaka A, Dietrich PJ, Fitch B, Raymond JR and Ford AP (2015) Isoproterenol acts as a biased agonist of the alpha-1A-adrenoceptor that selectively activates the MAPK/ERK pathway. PLoS One 10(1): e0115701.

Doi M, Yano M, Kobayashi S, Kohno M, Tokuhisa T, Okuda S, Suetsugu M, Hisamatsu Y, Ohkusa T and Kohno M (2002) Propranolol prevents the development of heart failure by restoring FKBP12. 6-mediated stabilization of ryanodine receptor. Circulation 105(11): 1374-1379.

Fagerholm V, Scheinin M and Haaparanta M (2008) α2A-Adrenoceptor antagonism increases insulin secretion and synergistically augments the insulinotropic effect of glibenclamide in mice. British journal of pharmacology 154(6): 1287-1296.

Farzam K and Jan A (2023) Beta blockers, in StatPearls [Internet], StatPearls Publishing.

Gafni J, Munsch JA, Lam TH, Catlin MC, Costa LG, Molinski TF and Pessah IN (1997) Xestospongins: potent membrane permeable blockers of the inositol 1, 4, 5-trisphosphate receptor. Neuron 19(3): 723-733.

Gonzales AL, Amberg GC and Earley S (2010) Ca^{2+} release from the sarcoplasmic reticulum is required for sustained TRPM4 activity in cerebral artery smooth muscle cells. American Journal of Physiology-Cell Physiology 299(2): C279-C288.

Guerrero-Hernández A, Sánchez-Vázquez VH, Martínez-Martínez E, Sandoval-Vázquez L, Perez-Rosas NC, Lopez-Farias R and Dagnino-Acosta A (2020) Sarco-endoplasmic reticulum calcium release model based on changes in the luminal calcium content. Calcium Signaling: 337-370.

Hain J, Onoue H, Mayrleitner M, Fleischer S and Schindler H (1995) Phosphorylation Modulates the Function of the Calcium Release Channel of Sarcoplasmic Reticulum from Cardiac Muscle (∗). Journal of Biological Chemistry 270(5): 2074-2081.

Hashim M, Yokoi N, Takahashi H, Gheni G, Okechi OS, Hayami T, Murao N, Hidaka S, Minami K and Mizoguchi A (2018) Inhibition of SNAT5 induces incretin-responsive state from incretin-unresponsive state in pancreatic β-cells: study of β-cell spheroid clusters as a model. Diabetes 67(9): 1795-1806.

Henquin, J. C. (2021) Non-glucose modulators of insulin secretion in healthy humans:(dis) similarities between islet and in vivo studies. Metabolism 122: 154821.

Holz GG, Leech CA, Heller RS, Castonguay M and Habener JF (1999) cAMP-dependent mobilization of intracellular Ca^{2+} stores by activation of ryanodine receptors in pancreatic β-cells: a Ca^{2+} signaling system stimulated by the insulinotropic hormone glucagon-like peptide-1-(7–37). Journal of Biological Chemistry 274(20): 14147-14156.

Imura H, Kato Y, Ikeda M, Morimoto M and Yawata M (1971) Effect of adrenergic-blocking or-stimulating agents on plasma growth hormone, immunoreactive insulin, and blood free fatty acid levels in man. The Journal of Clinical Investigation 50(5): 1069-1079.

Islam MS (2002) The ryanodine receptor calcium channel of β-cells: molecular regulation and physiological significance. Diabetes 51(5): 1299-1309.

Islam MS, Leibiger I, Leibiger B, Rossi D, Sorrentino V, Ekström TJ, Westerblad H, Andrade FH and Berggren P-O (1998) In situ activation of the type 2 ryanodine receptor in pancreatic beta cells requires cAMP-dependent phosphorylation. Proceedings of the National Academy of Sciences 95(11): 6145-6150.

Iwasaki M, Minami K, Shibasaki T, Miki T, Miyazaki Ji and Seino S (2010) Establishment of new clonal pancreatic β-cell lines (MIN6-K) useful for study of incretin/cyclic adenosine monophosphate signaling. Journal of Diabetes Investigation 1(4): 137-142.

Kagiyama N, Ikeda T, and Nomura T (2006) Japanese Guidelines and regulations for scientific and ethical animal experimentation. In Vivo Models of Inflammation: Volume I, 187-191

Kerns II W (2007) Management of β-adrenergic blocker and calcium channel antagonist toxicity. Emergency medicine clinics of North America 25(2): 309-331.

Kim T-E, Kang J-S, An W and Sohn JH (2022) Systemic exposure to propranolol in patients with chronic liver disease and its correlation with portal blood flow. Frontiers in Medicine 9: 973606.

Kyriazis GA, Soundarapandian MM and Tyrberg B (2012) Sweet taste receptor signaling in beta cells mediates fructose-induced potentiation of glucose-stimulated insulin secretion. Proceedings of the National Academy of Sciences 109(8): E524-E532.

Lacey, R. J., Cable, H. C., James, R. F. L., London, N. J. M., Scarpello, J. H. B., and Morgan, N. G. (1993) Concentration-dependent effects of adrenaline on the profile of insulin secretion from isolated human islets of Langerhans. Journal of endocrinology 138(3): 555-563.

Li G-f, Wang K, Chen R, Zhao H-r, Yang J and Zheng Q-s (2012) Simulation of the pharmacokinetics of bisoprolol in healthy adults and patients with impaired renal function using whole-body physiologically based pharmacokinetic modeling. Acta Pharmacologica Sinica 33(11): 1359-1371.

Loubatières A, Mariani M, Sorel G and Savi L (1971) The action of beta-adrenergic blocking and stimulating agents on insulin secretion. Characterization of the type of beta receptor. Diabetologia 7(3): 127-132.

Louiset E, Duparc C, Lenglet S, Gomez-Sanchez CE and Lefebvre H (2017) Role of cAMP/PKA pathway and T-type calcium channels in the mechanism of action of serotonin in human adrenocortical cells. Molecular and cellular endocrinology 441: 99-107.

Marx SO, Reiken S, Hisamatsu Y, Jayaraman T, Burkhoff D, Rosemblit N and Marks AR (2000) PKA phosphorylation dissociates FKBP12. 6 from the calcium release channel (ryanodine receptor): defective regulation in failing hearts. Cell 101(4): 365-376.

Murao N, Morikawa R, Seino Y, Shimomura K, Maejima Y, Ohno T, Yokoi N, Yamada Y and Suzuki A (2024a) Pyruvate kinase modulates the link between β-cell fructose metabolism and insulin secretion. bioRxiv: 2024.2008. 2015.608033.

Murao N, Morikawa R, Seino Y, Shimomura K, Maejima Y, Yamada Y and Suzuki A (2024b) Sildenafil amplifies calcium influx and insulin secretion in pancreatic β cells. Physiological Reports 12(11): e16091.

Nauck MA, Müller TD (2023) Incretin hormones and type 2 diabetes. Diabetologia 66(10): 1780-1795.

Oduori OS, Murao N, Shimomura K, Takahashi H, Zhang Q, Dou H, Sakai S, Minami K, Chanclon B and Guida C (2020) Gs/Gq signaling switch in β cells defines incretin effectiveness in diabetes. The Journal of clinical investigation 130(12): 6639-6655.

Ohno T, Miyasaka Y, Yoshida K, Kobayashi M, Horio F, Yokoi N, Mizuno M and Ikegami H (2022) A novel model mouse for type 2 diabetes mellitus with early onset and persistent hyperglycemia. Experimental Animals 71(4): 510-518.

Palmer RK, Atwal K, Bakaj I, Carlucci-Derbyshire S, Buber MT, Cerne R, Cortés RY, Devantier HR, Jorgensen V and Pawlyk A (2010) Triphenylphosphine oxide is a potent and selective inhibitor of the transient receptor potential melastatin-5 ion channel. Assay and drug development technologies 8(6): 703-713.

Patt J, Alenfelder J, Pfeil EM, Voss JH, Merten N, Eryilmaz F, Heycke N, Rick U, Inoue A and Kehraus S (2021) An experimental strategy to probe Gq contribution to signal transduction in living cells. Journal of Biological Chemistry 296.

Paul A (2021) Adrenergic Antagonists. Introduction to Basics of Pharmacology and Toxicology: Volume 2: Essentials of Systemic Pharmacology: From Principles to Practice: 55-65.

Pian-Smith MC, Wiedenkeller DE and Sharp GW (1986) Paradoxical potentiation of stimulated insulin release by dantrolene in rat pancreatic islets. Pancreas 1(6): 501-508.

Plant T and Henquin J-C (1990) Phentolamine and yohimbine inhibit ATP-sensitive K+ channels in mouse pancreatic beta-cells. British journal of pharmacology 101(1): 115.

Porte D (1969) Sympathetic regulation of insulin secretion: its relation to diabetes mellitus. Archives of internal medicine 123(3): 252-260.

Porte Jr D (1967) Beta adrenergic stimulation of insulin release in man. Diabetes 16(3): 150-155.

Proks P and Ashcroft FM (1997) Phentolamine block of K_{ATP} channels is mediated by Kir6. 2. Proceedings of the National Academy of Sciences 94(21): 11716-11720.

Reiken S, Wehrens XH, Vest JA, Barbone A, Klotz S, Mancini D, Burkhoff D and Marks AR (2003) β-blockers restore calcium release channel function and improve cardiac muscle performance in human heart failure. Circulation 107(19): 2459-2466.

Rorsman P and Ashcroft FM (2018) Pancreatic β-cell electrical activity and insulin secretion: of mice and men. Physiological reviews 98(1): 117-214.

Schuit F and Pipeleers D (1986) Differences in adrenergic recognition by pancreatic A and B cells. Science 232(4752): 875-877.

Seino S and Shibasaki T (2005) PKA-dependent and PKA-independent pathways for cAMP-regulated exocytosis. Physiological reviews 85(4): 1303-1342.

Shan J, Betzenhauser MJ, Kushnir A, Reiken S, Meli AC, Wronska A, Dura M, Chen B-X and Marks AR (2010a) Role of chronic ryanodine receptor phosphorylation in heart failure and β-adrenergic receptor blockade in mice. The Journal of clinical investigation 120(12): 4375-4387.

Shan J, Kushnir A, Betzenhauser MJ, Reiken S, Li J, Lehnart SE, Lindegger N, Mongillo M, Mohler PJ and Marks AR (2010b) Phosphorylation of the ryanodine receptor mediates the cardiac fight or flight response in mice. The Journal of clinical investigation 120(12): 4388-4398.

Sharifpour A, Sadeghi M, Zakariaei Z and Soleymani M (2022) Seizures and irreversible cardiogenic shock following propranolol poisoning: report of 2 cases and literature review. Clinical Medicine Insights: Case Reports 15: 11795476221126981.

Sharma A, Rahman G, Gorelik J and Bhargava A (2023) Voltage-gated T-type calcium channel modulation by kinases and phosphatases: the old ones, the new ones, and the missing ones. Cells 12(3): 461.

Shigeto M, Ramracheya R, Tarasov AI, Cha CY, Chibalina MV, Hastoy B, Philippaert K, Reinbothe T, Rorsman N and Salehi A (2015) GLP-1 stimulates insulin secretion by PKC-dependent TRPM4 and TRPM5 activation. The Journal of clinical investigation 125(12): 4714-4728.

Sluga N, Križančić Bombek L, Kerčmar J, Sarikas S, Postić S, Pfabe J, Skelin Klemen M, Korošak D, Stožer A and Slak Rupnik M (2022) Physiological levels of adrenaline fail to stop pancreatic beta cell activity at unphysiologically high glucose levels. Frontiers in Endocrinology 13: 1013697.

Straub SG, Sharp GW (2012) Evolving insights regarding mechanisms for the inhibition of insulin release by norepinephrine and heterotrimeric G proteins. American Journal of Physiology-Cell Physiology 302(12): C1687-C1698.

Taegtmeyer AB, Haschke M, Tchambaz L, Buylaert M, Tschöpl M, Beuers U, Drewe J and Krähenbühl S (2014) A study of the relationship between serum bile acids and propranolol pharmacokinetics and pharmacodynamics in patients with liver cirrhosis and in healthy controls. PloS One 9(6): e97885.

Takasaki J, Saito T, Taniguchi M, Kawasaki T, Moritani Y, Hayashi K and Kobori M (2004) A novel Gαq/11-selective inhibitor. Journal of Biological Chemistry 279(46): 47438-47445.

Tengholm A and Gylfe E (2017) cAMP signaling in insulin and glucagon secretion. Diabetes, obesity and metabolism 19: 42-53.

Tjandrawinata RR, Setiawati E, Yunaidi DA, Santoso ID, Setiawati A and Susanto LW (2012) Bioequivalence study of two formulations of bisoprolol fumarate film-coated tablets in healthy subjects. Drug design, development and therapy: 311-316.

Varney MJ and Benovic JL (2024) The Role of G Protein–Coupled Receptors and Receptor Kinases in Pancreatic β-Cell Function and Diabetes. Pharmacological Reviews 76(2): 267-299.

Watts SW, Fink GD, Silver PJ and Cushing DJ (2000) Interaction of the β adrenergic receptor antagonist bucindolol with serotonergic receptors. Journal of cardiovascular pharmacology 35(1): 29-36.

Wehrens XH, Lehnart SE, Reiken S, Vest JA, Wronska A and Marks AR (2006) Ryanodine receptor/calcium release channel PKA phosphorylation: a critical mediator of heart failure progression. Proceedings of the National Academy of Sciences 103(3): 511-518.

Zhang Z, Zhao Z, Margolskee R and Liman E (2007) The transduction channel TRPM5 is gated by intracellular calcium in taste cells. Journal of Neuroscience 27(21): 5777-5786.

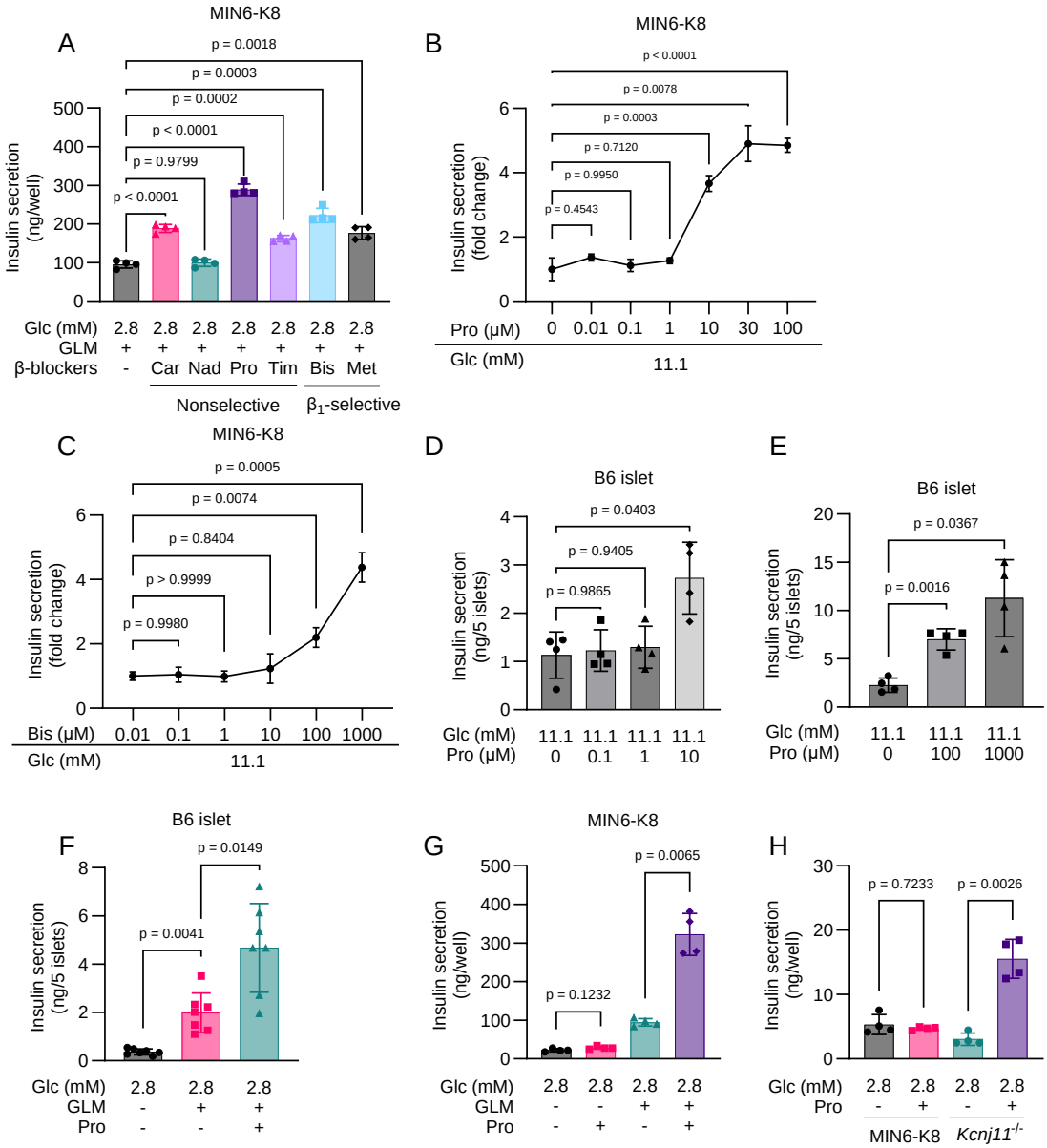

Figure 1.

Figure 1. Effect of β-blockers on glucose- and glimepiride-induced insulin secretion.

A. Effect of various non-selective and β1-selective β-blockers on glimepiride-induced insulin secretion in MIN6-K8 cells. Car, carteolol; Nad, nadolol; Pro, propranolol; Tim, timolol; Bis, bisoprolol; Met, metoprolol. All β-blockers were used at a concentration of 100 μM. n = 4.

B. Dose-dependent effect of propranolol on glucose-induced insulin secretion in MIN6-K8 cells. n = 4.

C. Dose-dependent effect of bisoprolol on glucose-induced insulin secretion in MIN6-K8 cells. n = 4.

D. –E. Dose-dependent effect of propranolol on glucose-induced insulin secretion in B6 mouse islets. One mouse was used for each experiment. n = 4.

F. Effect of propranolol on glimepiride-induced insulin secretion in B6 mouse islets. n = 7.

G. Requirement of glimepiride for propranolol-stimulated insulin secretion at 2.8 mM glucose. n = 4.

H. Effect of K_{ATP} channel deficiency on propranolol-stimulated insulin secretion. n = 4.

Data are presented as mean ± standard deviation (SD). Glc, glucose. The reagents were added to achieve the following final concentrations unless otherwise specified: glimepiride (GLM), 1 μM; and propranolol (Pro), 100 μM. Statistical comparisons were performed using Welch's one-way ANOVA with Dunnett's post-hoc test.

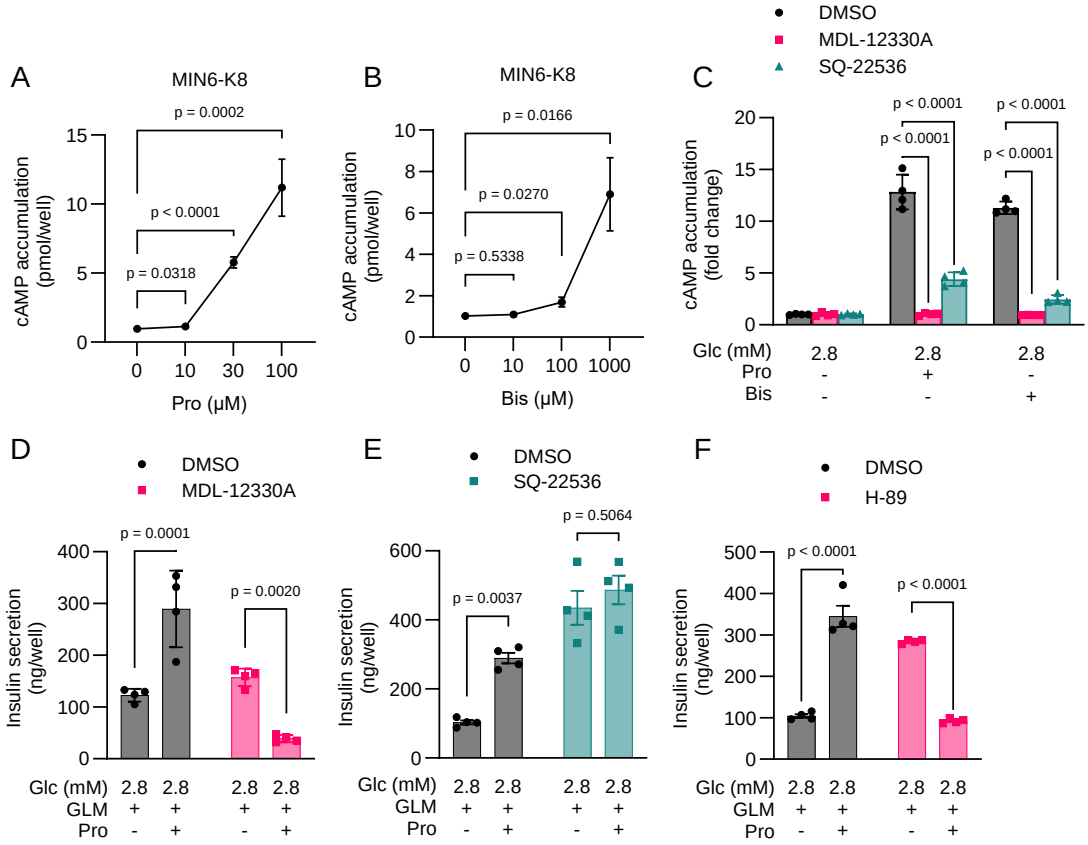

Figure 2.

Figure 2. Characterization of β-blocker-stimulated cAMP production and insulin secretion in MIN6-K8 cells.

A. Effect of propranolol on intracellular cAMP accumulation. n = 4.

B. Effect of bisoprolol on intracellular cAMP accumulation. n = 4.

C. Effects of AC inhibitors on β-blocker-stimulated cAMP production. n = 4. The data are presented as fold change over 2.8 mM glucose alone. See Figure S1B for the original values.

D. –E. Effects of AC inhibitors on propranolol-SIS. MDL-12330A and SQ-22536 were used for D and E, respectively. n = 4.

F. Effect of H-89 on propranolol-SIS. n = 4.

All experiments were performed using MIN6-K8 cells. Data are presented as mean ± SD. Glc, glucose. The reagents were added to achieve the following final concentrations unless otherwise specified: glimepiride (GLM) – 1 μM, propranolol (Pro) – 100 μM, bisoprolol (Bis) – 100 μM, MDL-12330A – 10 μM, SQ-22536 – 1 mM, and H-89 – 10 μM. Statistical comparisons were made using Welch's one-way ANOVA with Dunnett's post-hoc test for A and B, and two-way ANOVA with Šídák's post-hoc test for C – F.

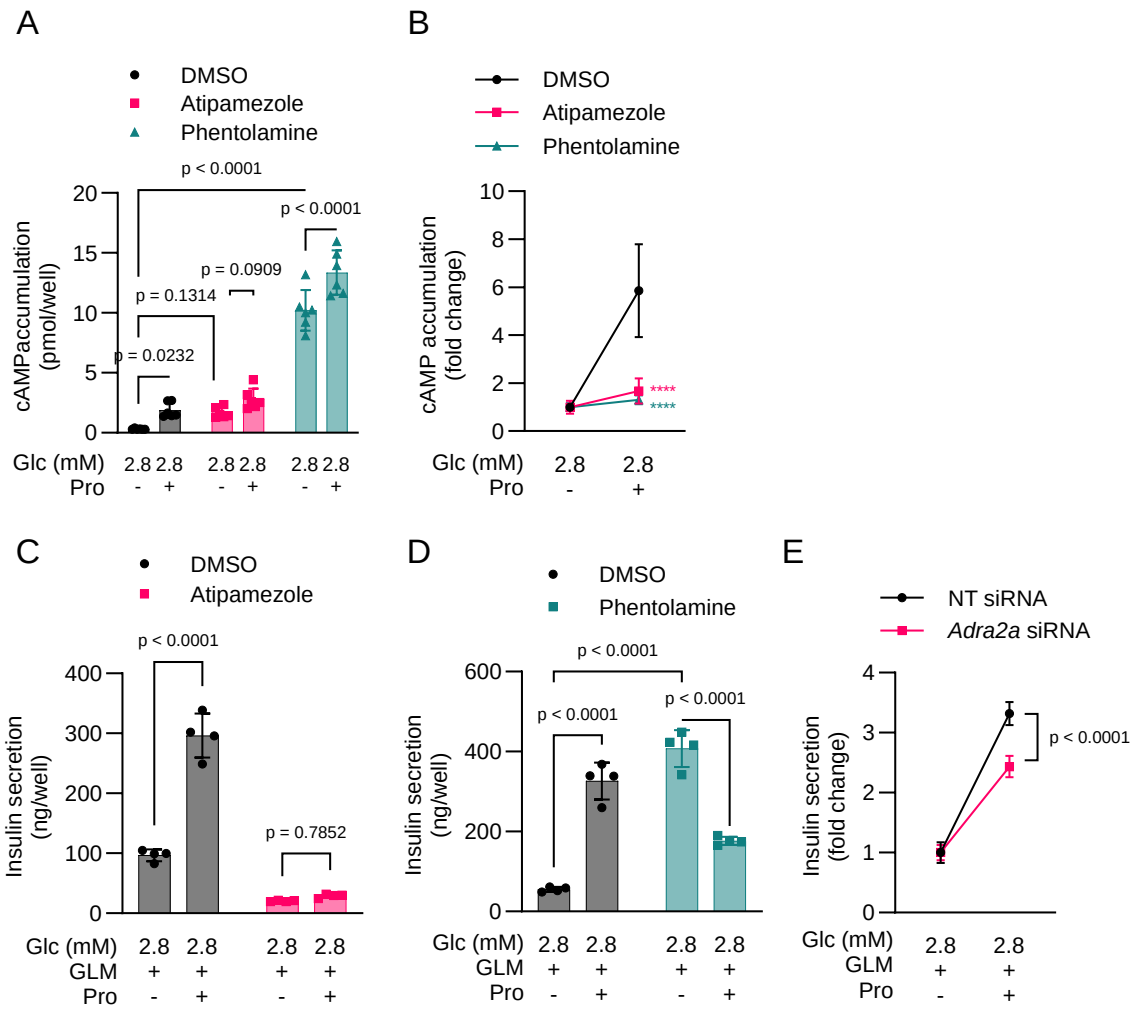

Figure 3.

Figure 3. Effect of α2-adrenoceptor inhibition on propranolol-stimulated cAMP in MIN6-K8 cells.

A. –B. Effects of α2-adrenoceptor inhibitors on intracellular cAMP accumulation. n = 6. The data **are** presented **as** original value in A and as fold change over 2.8 mM glucose alone in B.

C. –D. Effects of α2-adrenoceptor inhibitors on propranolol-SIS. n = 4. Phentolamine and atipamezole were used in C and D, respectively. n = 4.

E. Effect of α2A-adrenoceptor knockdown on propranolol-SIS. n = 4. The data are presented as fold change. See Figure S2I for the original values.

All experiments were performed using MIN6-K8 cells. Data are presented as mean ± SD. Glc, glucose. The reagents were added to achieve the following final concentrations, unless otherwise specified: glimepiride (GLM), 1 μM; propranolol (Pro), 100 μM; phentolamine, 100 μM; and atipamezole, 250 μM. Statistical comparisons were made using Welch's one-way ANOVA with Dunnett's post-hoc test for B, two-way ANOVA with Šídák's post-hoc test for A and C, two-way ANOVA with uncorrected Fisher's LSD for D, and Welch's unpaired two-tailed t-test for E. $^{****}p < 0.0001$ versus DMSO.

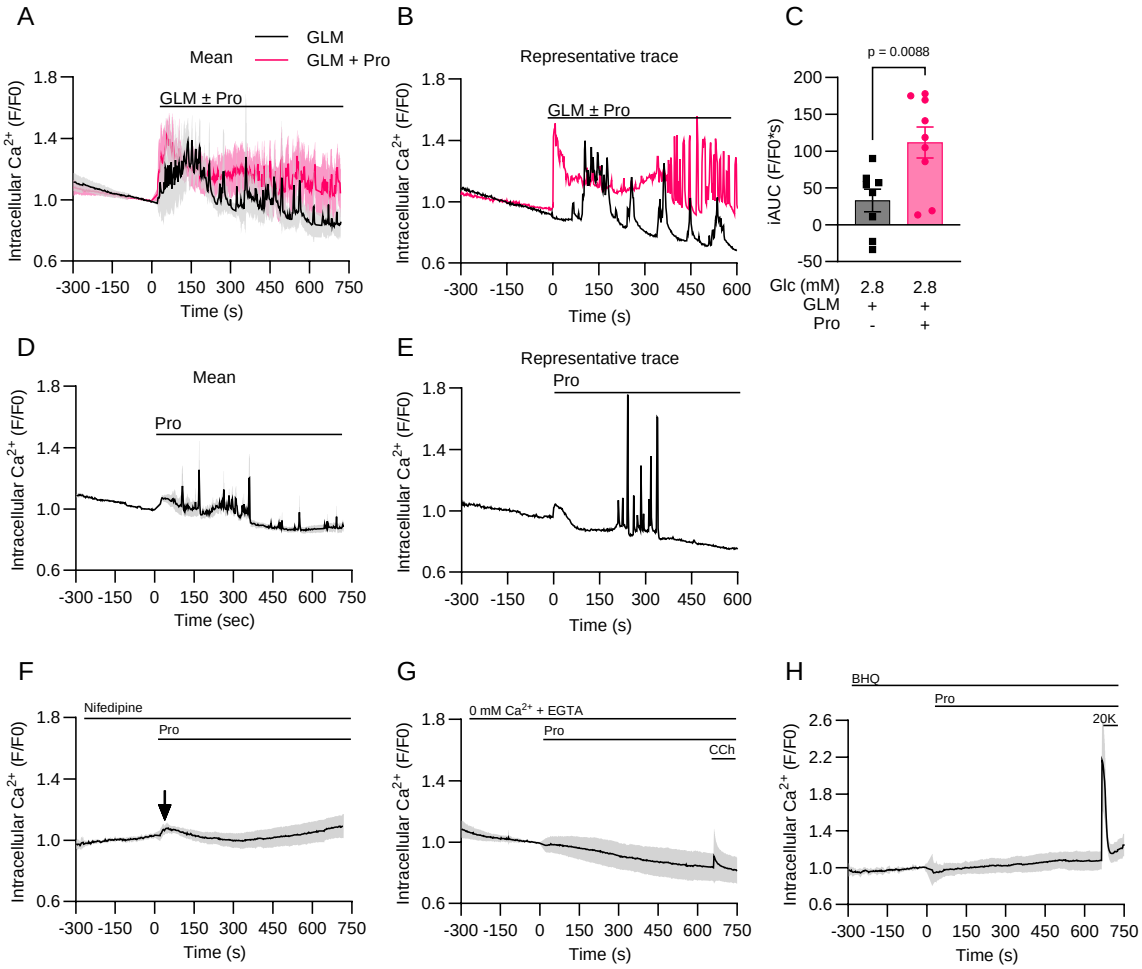

Figure 4.

Figure 4. Characterization of propranolol-stimulated Ca^{2+} response in MIN6-K8 cells. Intracellular Ca^{2+} levels were measured using Fluo-4. All experiments were performed using MIN6-K8 cells in the presence of 2.8 mM glucose. The averaged time courses of normalized fluorescence intensity (F/F0) are indicated in A, D, and F–H. Representative traces are indicated in B and E.

A. –C. Effects of propranolol on the glimepiride-induced Ca^{2+} response. GLM: n = 8; GLM + Pro: n = 9. C, The magnitude of Ca^{2+} responses was quantified as the incremental area under the curve (iAUC).

D. –E. Propranolol-stimulated Ca^{2+} response. n = 7.

F. Effect of nifefdipine (100 μM) on the glimepiride-induced Ca^{2+} response. n = 12.

G. Propranolol-stimulated Ca^{2+} response in extracellular Ca^{2+}-free conditions. n = 17. EGTA: 100 μM. Carbachol (CCh, 50 μM) was added as a positive control at the end of the recording. The black arrow indicates the $[Ca^{2+}]_i$ increase at 0 min.

H. Effect of BHQ (15 μM) on glimepiride-induced Ca^{2+} response. n = 19. 20 mM K^+ (20K) was added as a positive control at the end of the recording.

Data are presented as mean ± SD. Glc, glucose. The reagents were added to achieve the following final concentrations unless otherwise specified: glimepiride (GLM), 1 μM; and propranolol (Pro), 100 μM. Statistical comparisons were made using Welch's unpaired two-tailed t-test for C.

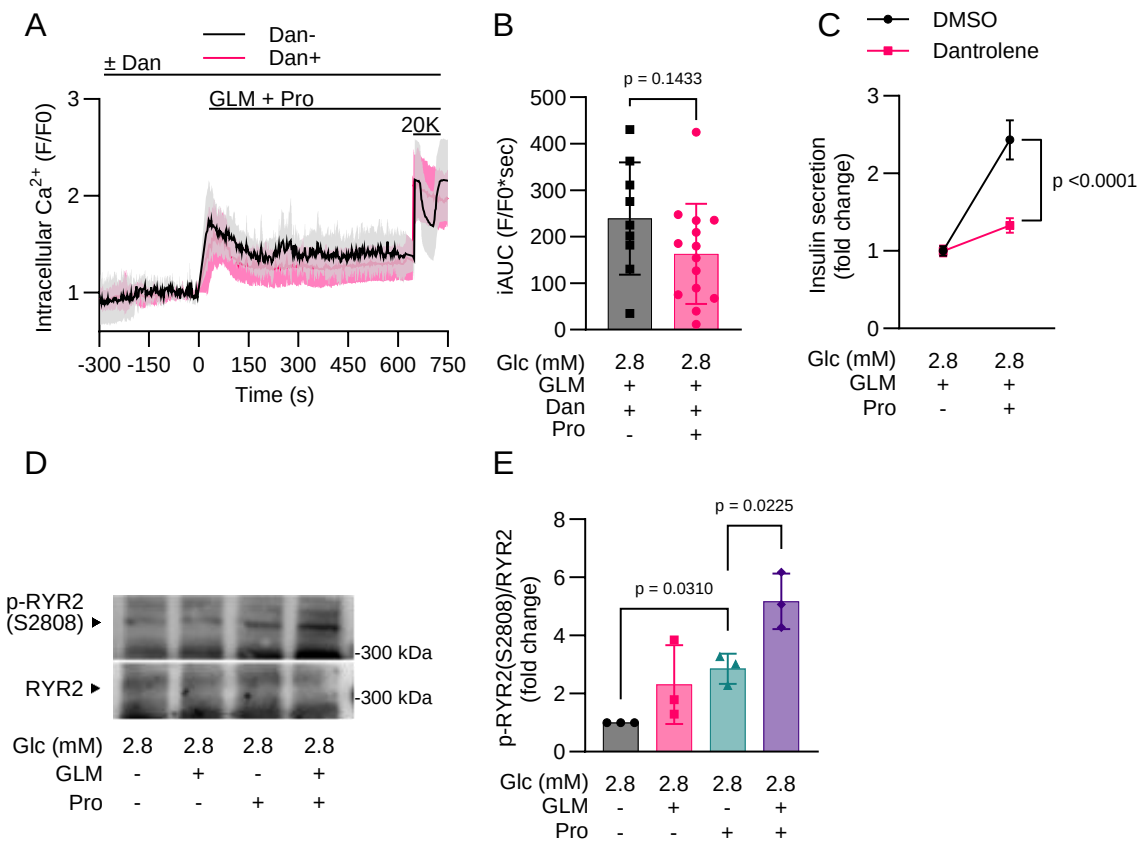

Figure 5.

Figure 5. Involvement of ryanodine receptor in propranolol-stimulated Ca^{2+} response in MIN6-K8 cells.

A. –B. Effect of dantrolene on the propranolol-stimulated Ca^{2+} response in the presence of glimepiride. The averaged time courses of the normalized fluorescence intensity of Fluo-4 (F/F0) are indicated. Dan-: n = 9; Dan+: n = 14. GLM + Pro: n = 9. C, 20 mM K^+ (20K) was added as a positive control at the end of the recording. The magnitude of Ca^{2+} responses was quantified as the incremental area under the curve (iAUC) between 0 and 600 s.

C. Effect of dantrolene on propranolol-SIS. The data are presented as fold change. See Figure S3D for the original values.

D. –E. The effects of glimepiride and propranolol on RYR2 phosphorylation at Ser-2808 were assessed by immunoblotting. The intensity of phosphorylated RYR2 (Ser-2808) was normalized to total RYR2 (Ser-2808) and expressed as fold change over 2.8 mM glucose in E. n = 3.

All experiments were performed using MIN6-K8 cells in the presence of 2.8 mM glucose. Data are presented as mean ± SD. The reagents were added to achieve the following final concentrations, unless otherwise specified: dantrolene (Dan), 100 μM; glimepiride (GLM), 1 μM; and propranolol (Pro), 100 μM. Statistical comparison was made using Welch's unpaired two-tailed t-test for B and C, and Welch's one-way ANOVA with Dunnett's post-hoc test for E.

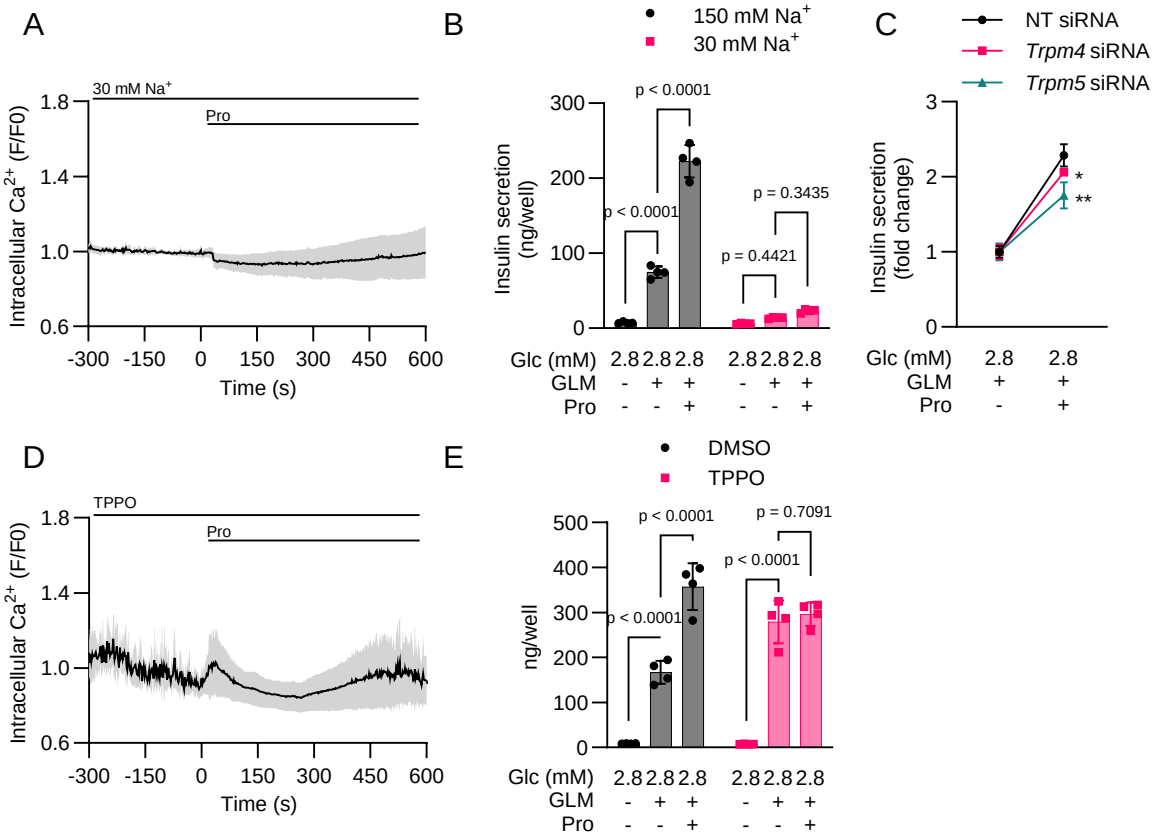

Figure 6.

Figure 6. Involvement of TRPM4 and TRPM5 in propranolol-stimulated Ca^{2+} response in MIN6-K8 cells.

A. Effect of low extracellular sodium concentration (30 mM) on the propranolol-stimulated Ca^{2+} response. The averaged time course of the normalized fluorescence intensity of Fluo-4 (F/F0) is indicated. n = 12.

B. Effect of low extracellular sodium concentration (30 mM) on propranolol-SIS. n = 4.

C. Effects of *Trpm4* and *Trpm5* knockdown on propranolol-SIS. n = 4. The data are presented as fold change. See Figure S4C for the original values. $^{*}p < 0.05$, $^{**}p < 0.01$ versus NT (non-targeting) siRNA.

D. Effect of triphenylphosphine oxide on propranolol-stimulated Ca^{2+} response. The averaged time course of the normalized fluorescence intensity of Fluo-4 (F/F0) is indicated. n = 12.

E. Effect of triphenylphosphine oxide on propranolol-SIS. n = 4.

All experiments were performed using MIN6-K8 cells in the presence of 2.8 mM glucose. Data are presented as mean ± SD. The reagents were added at the following final concentrations unless otherwise specified: glimepiride (GLM), 1 μM; propranolol (Pro), 100 μM; and triphenylphosphine oxide (TPPO), 100 μM. Statistical comparisons were made using Welch's one-way ANOVA with Dunnett's post-hoc test for C and two-way ANOVA with Šídák's post-hoc test for B and E.

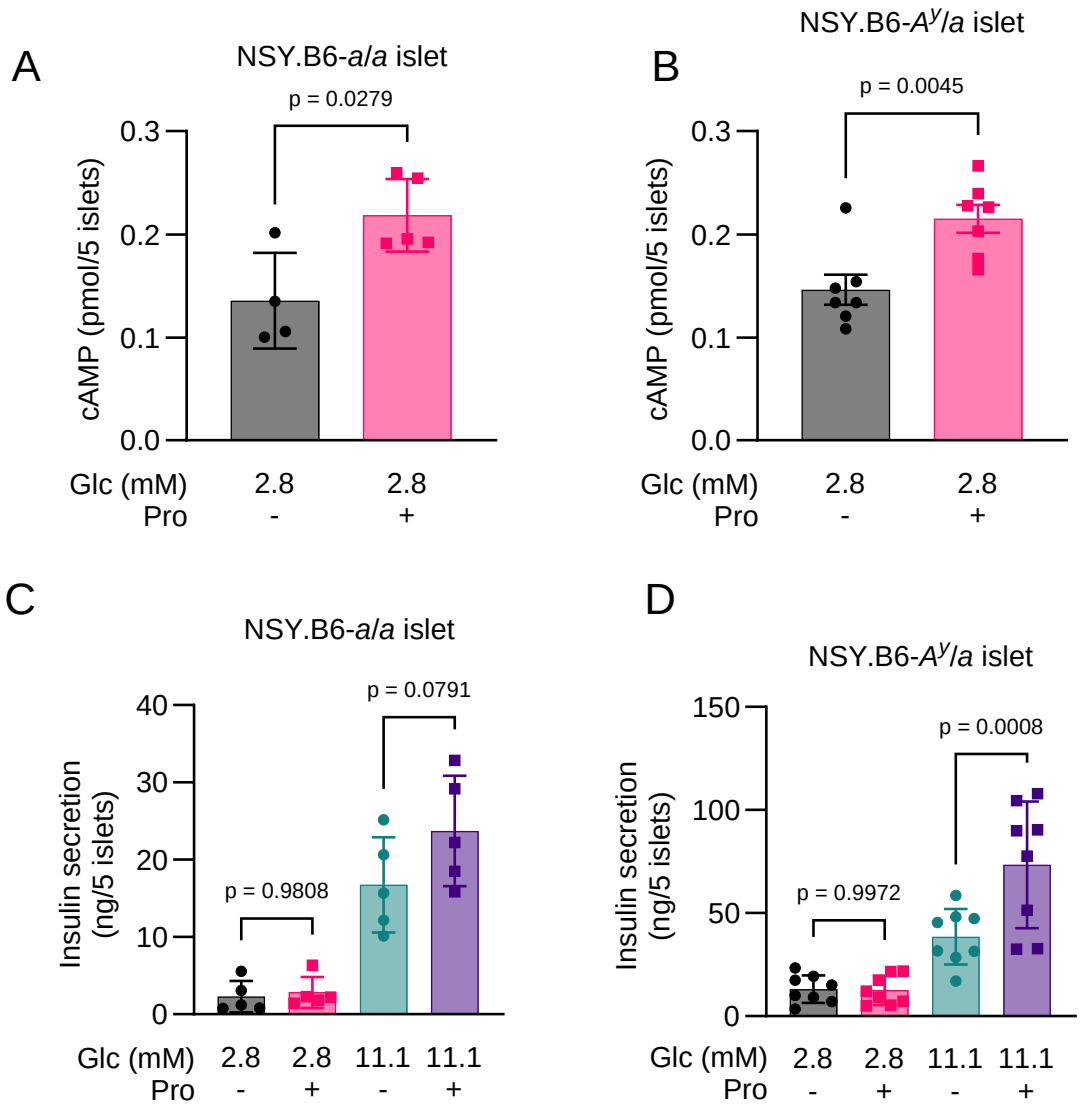

Figure 7.

Figure 7. Propranolol stimulated cAMP production and insulin secretion in islets of normal and diabetic mice.

A. –B. Effect of propranolol on intra-islet cAMP levels A, NSY.B6-*a*/*a* mouse islets. Islets were pooled from two mice. n = 4–5. B, NSY.B6-A^y/*a* mouse islets. Islets were pooled from two mice. n = 7.

C. –D. Effect of propranolol on insulin secretion. A, NSY.B6-*a*/*a* mouse islets. Islets were pooled from two mice. n = 5. B, NSY.B6-A^y/*a* mouse islets. Islets were pooled from two mice. n = 8.

Glc, glucose. Propranolol (Pro): 100 μM. Statistical comparisons were performed using Welch's unpaired two-tailed t-test for A and B, and Welch's one-way ANOVA with Dunnett's post-hoc test for C and D.

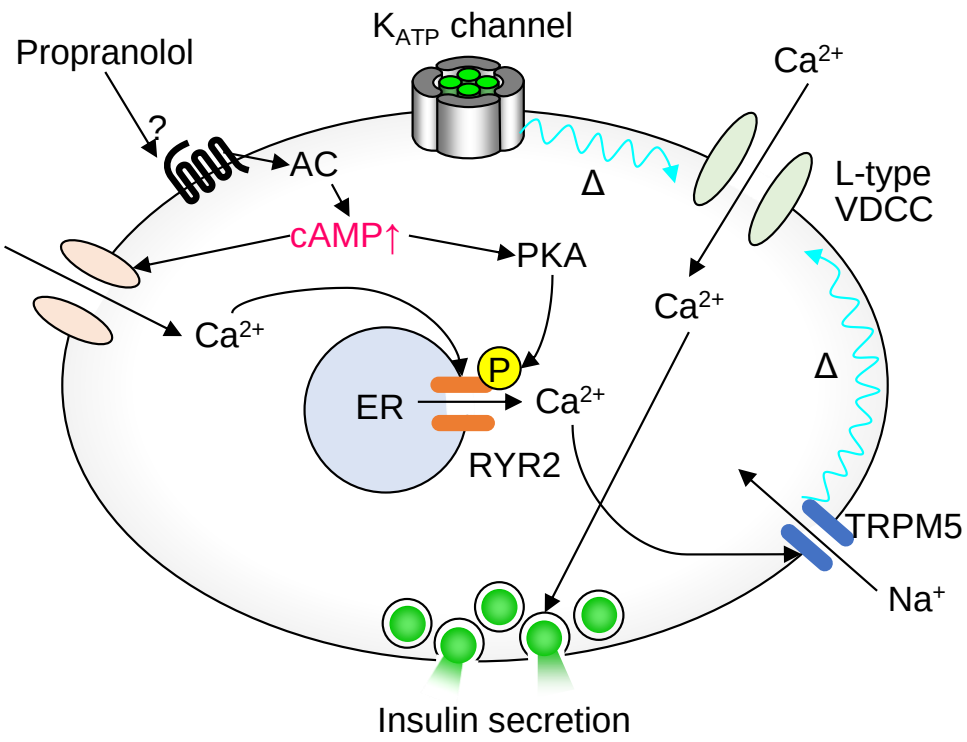

Figure 8.

Figure 8. Schematic overview of the mechanism of propranolol-stimulated insulin secretion in pancreatic β-cells.

Propranolol increases AC-mediated cAMP production via an unidentified mechanism, resulting in PKA activation. PKA induces RYR2 phosphorylation and extracellular Ca^{2+} influx, leading to CICR from the ER. CICR activates TRPM5, which augments β-cell electrical activity, extracellular Ca^{2+} influx through L-type VDCC, and insulin secretion. P, phosphorylation. Δ, depolarization.

		FPKM (n = 3)					
		MIN6-K8			B6 islet		
Adra1a	adrenergic receptor, alpha 1a	0.00	0.00	0.00	1.42	0.00	0.00
Adra1b	adrenergic receptor, alpha 1b	0.00	0.00	0.00	0.71	0.00	0.00
Adra1d	adrenergic receptor, alpha 1d	0.00	0.00	0.00	0.00	0.00	0.00
Adra2a	adrenergic receptor, alpha 2a	455.46	442.45	462.39	354.60	373.48	345.46
Adra2b	adrenergic receptor, alpha 2b	0.00	1.00	0.00	0.00	0.00	0.00
Adra2c	adrenergic receptor, alpha 2c	0.00	0.00	0.00	0.00	0.00	0.00
Adrb1	adrenergic receptor, beta 1	0.00	0.00	0.00	2.83	1.13	0.98
Adrb2	adrenergic receptor, beta 2	0.00	0.00	0.00	0.00	1.13	0.00
Adrb3	adrenergic receptor, beta 3	0.00	0.00	0.00	0.00	0.00	0.00

Table S1. Expression profiles of adrenoceptors in MIN6-K8 cells and B6 mouse islets.

Source data: DDBJ Sequence Read Archive (DRA) accession number DRA006332 (Hashim et al., 2018). n = 3 for each.

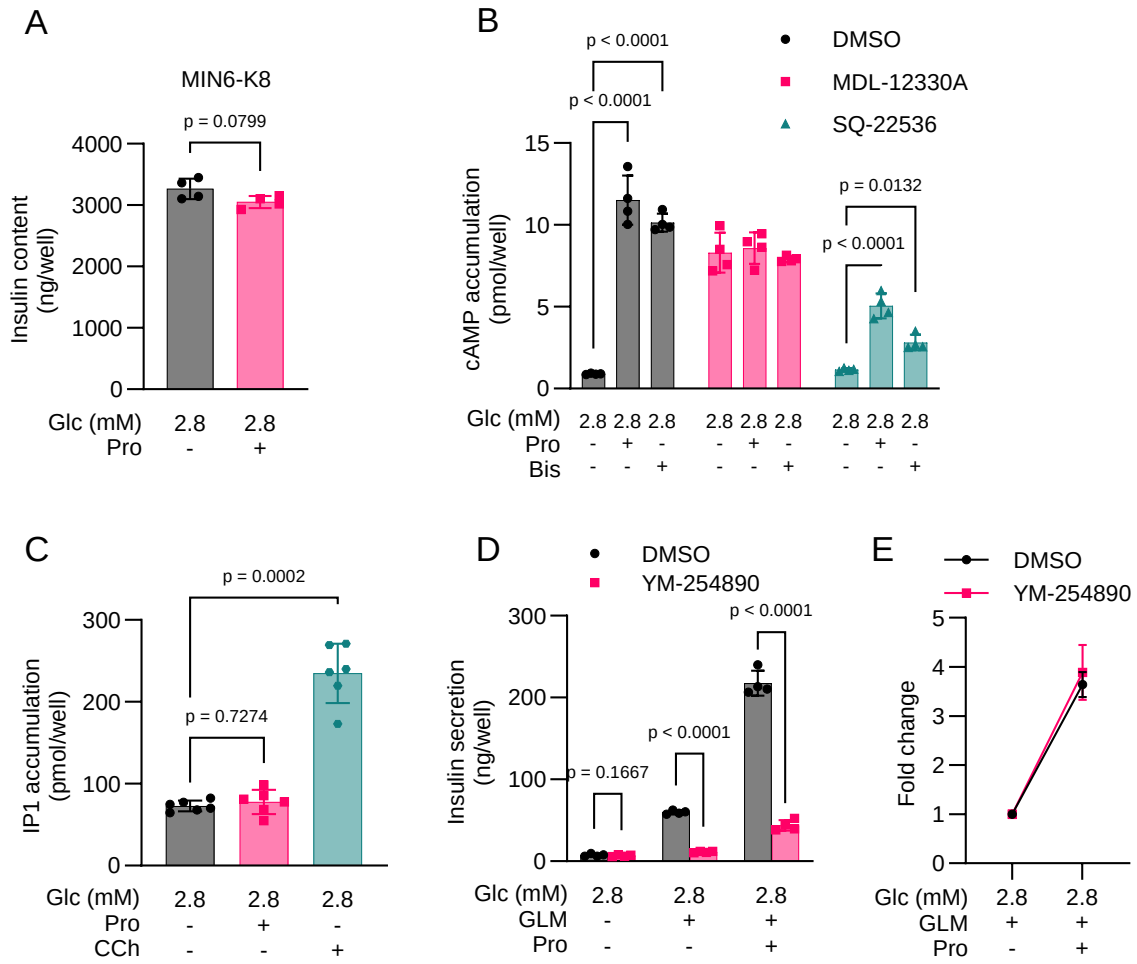

Figure S1.

Figure S1. Involvement of Gαs- and Gαq-GPCR signaling pathways in propranolol-stimulated insulin secretion in MIN6-K8 cells.

A. Effect of propranolol on intracellular insulin content. n = 4.
B. Effects of AC inhibitors on β-blocker-stimulated cAMP production. n = 4. Bisoprolol (Bis) – 100 μM, MDL-12330A – 10 μM, SQ-22536 – 1 mM.
C. Effect of propranolol on intracellular IP1 accumulation. n = 6. Carbachol (CCh, 50 μM) was used as the positive control.
D. –E. Effect of YM-254890 (100 nM) on propranolol-SIS. n = 4. The data are presented in their original value in C and as fold change over glimepiride in D.

All experiments were performed using MIN6-K8 cells in the presence of 2.8 mM glucose. The reagents were added to achieve the following final concentrations: glimepiride (GLM), 1 μM; and propranolol (Pro), 100 μM. Data are presented as mean ± SD. Statistical comparisons were made using two-way ANOVA with Šídák's post-hoc test for B, Welch's one-way ANOVA with Dunnett's post-hoc test for C, and Welch's unpaired two-tailed t-test for A and D.

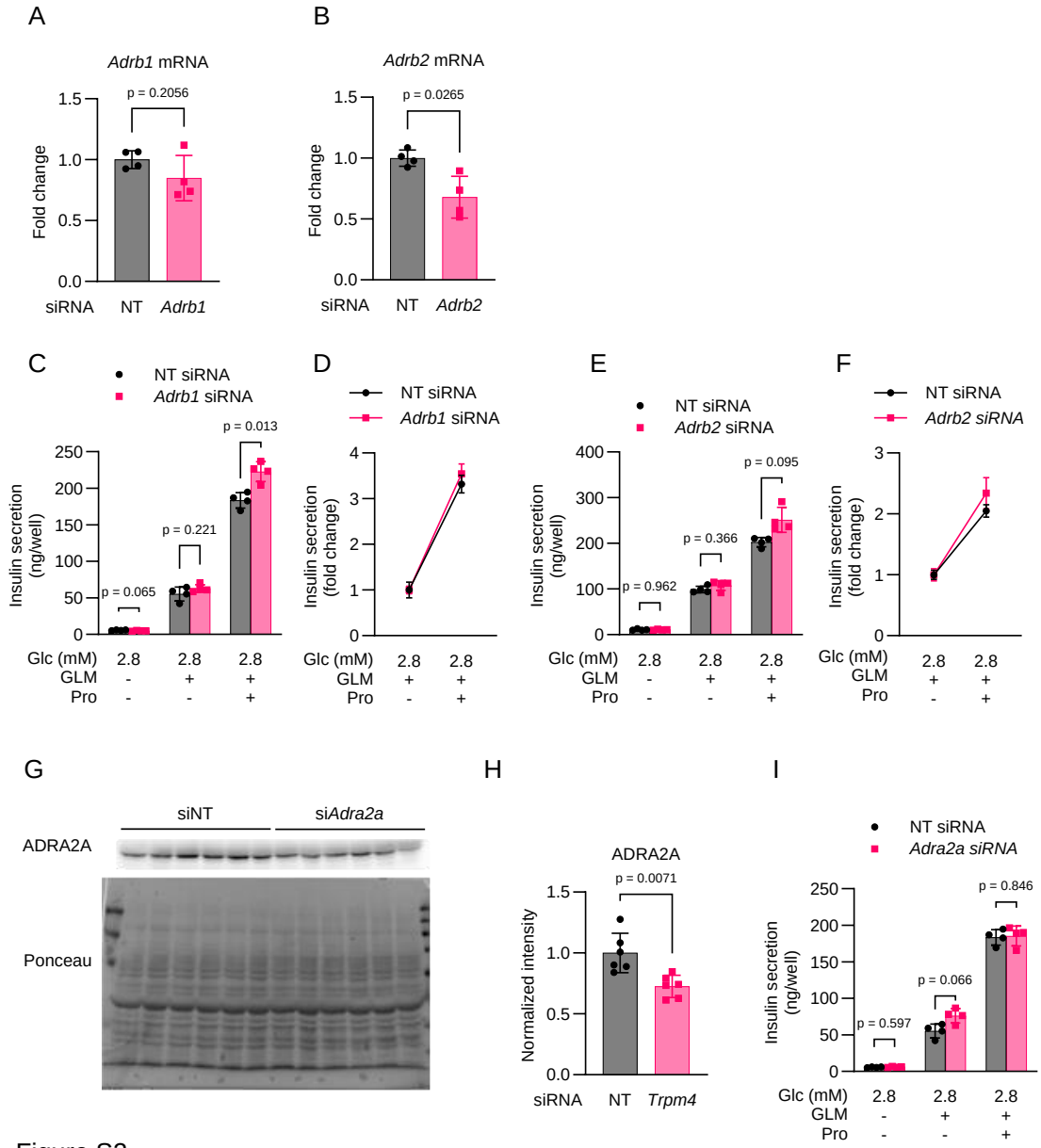

Figure S2.

Figure S2. Effects of adrenoceptor knockdown on propranolol-stimulated insulin secretion in MIN6-K8 cells.

A. –B. The knockdown efficiencies of *Adrb1* and *Adrb2* were assessed using RT-qPCR. The mRNA levels were normalized to those in siNT (non-targeting siRNA)-treated cells. n = 4.

C. –D. Effect of *Adrb1* knockdown on propranolol-SIS. n = 4. The data are presented in their original value in C and as fold change over glimepiride in D.

D. –F. Effect of *Adrb2* knockdown on propranolol-SIS. n = 4. The data are presented in their original value in F and as fold change over glimepiride in F.

G. –H. The knockdown efficiency of *Adra2a* was assessed by immunoblotting. The intensity of ADRA2A was normalized to that of total protein visualized by Ponceau-S staining and expressed as fold change over 2.8 mM glucose in H. n = 6.

I. Effect of *Adra2a* knockdown on propranolol-SIS. n = 4.

All experiments were performed using MIN6-K8 cells. Glc, glucose. Data are presented as the mean ± SD. Statistical comparisons were made using Welch's unpaired two-tailed t-test.

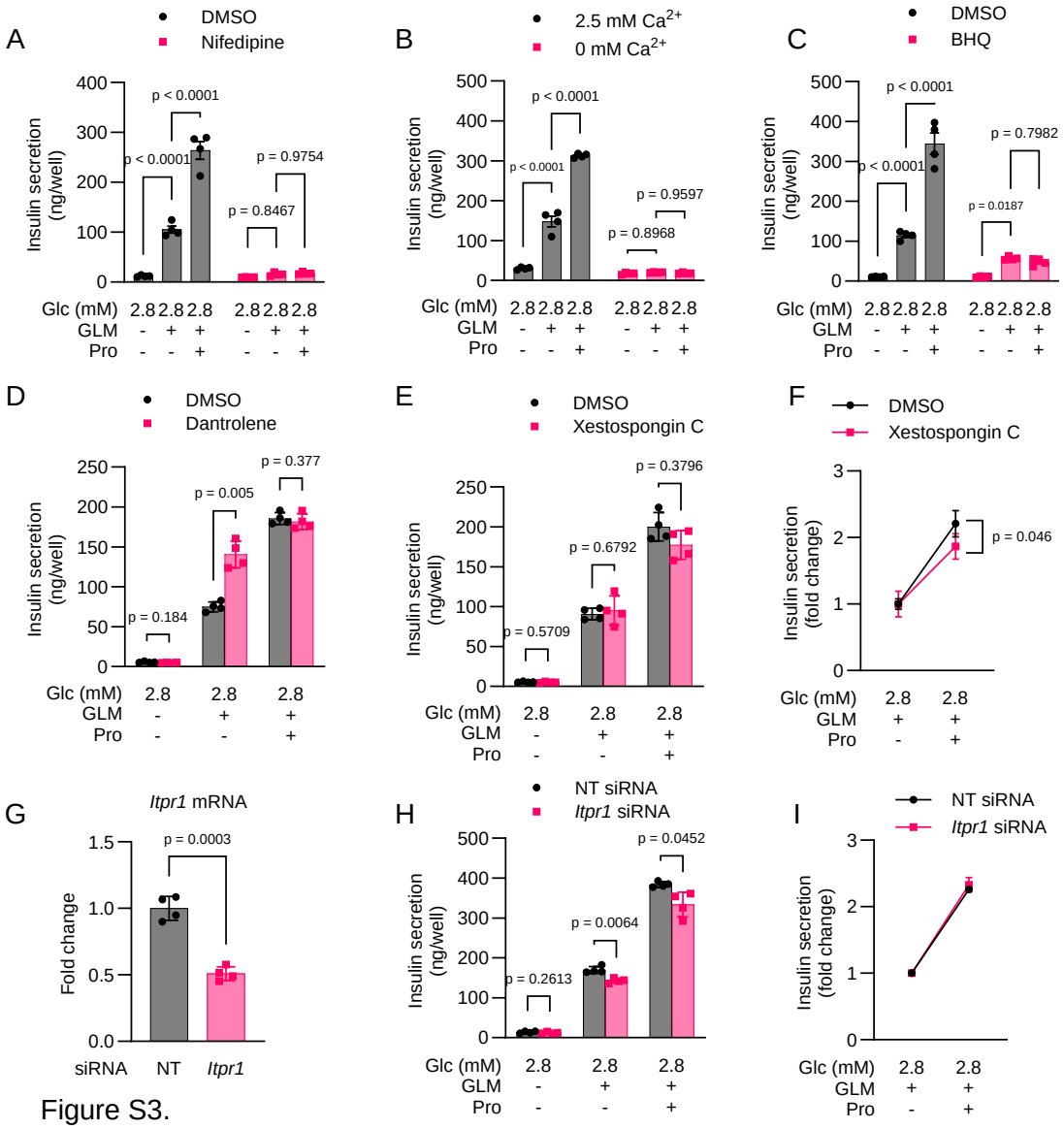

Figure S3.

Figure S3. Involvement of intracellular and extracellular Ca^{2+} in propranolol-stimulated insulin secretion in MIN6-K8 cells.

A. Effect of nifedipine (100 μM) on propranolol-SIS. n = 4.
B. Propranolol-SIS under extracellular Ca^{2+}-free conditions. n = 4. EGTA (100 μM) was added to the Ca^{2+}-free buffer.
C. Effect of BHQ (15 μM) on propranolol-SIS. n = 4.
D. Effect of dantrolene (100 μM) on propranolol-SIS. n = 4.
E. –F. Effect of xestospongin C (2 μM) on propranolol-SIS. n = 4. The data are presented in their original value in E and as fold change over glimepiride in F.
G. The knockdown efficiency of *Itpr1* was assessed using RT-qPCR. The mRNA levels were normalized to those in siNT (non-targeting siRNA)-treated cells. n = 4.
H. –I. Effect of *Itpr1* knockdown on propranolol-SIS. n = 4. The data are presented in their original value in H and as fold change over glimepiride in I.

All experiments were performed using MIN6-K8 cells. Glc, glucose. The reagents were added to achieve the following final concentrations: glimepiride (GLM), 1 μM; and propranolol (Pro), 100 μM. Data are presented as mean ± SD. Statistical comparisons were made using two-way ANOVA with Šídák's post-hoc test for A–C and Welch's unpaired two-tailed t-test for D–H.

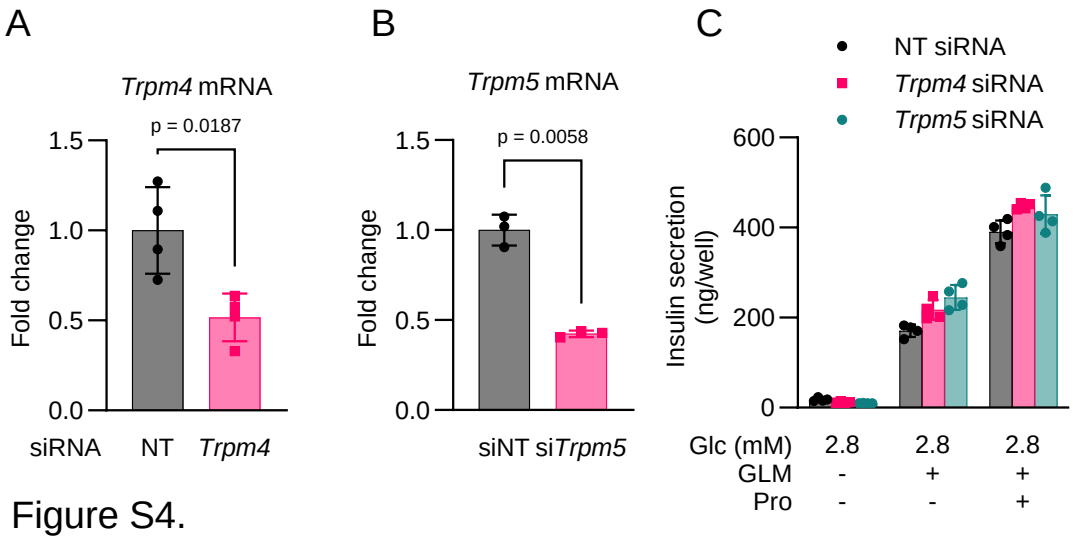

Figure S4. Effects of *Trpm4* and *Trpm5* knockdown on propranolol-stimulated insulin secretion in MIN6-K8 cells.

A. –B. The knockdown efficiencies of *Trpm4* and *Trpm5* were assessed using RT-qPCR. The mRNA levels were normalized to those in siNT (non-targeting siRNA)-treated cells. n = 4.
C. Effect of *Trpm4* and *Trpm5* knockdown on propranolol-SIS. n = 4.

All experiments were performed using MIN6-K8 cells. Glc, glucose. The reagents were added to achieve the following final concentrations: glimepiride (GLM), 1 μM; and propranolol (Pro), 100 μM. Data are presented as mean ± SD. Statistical comparisons were made using Welch's unpaired two-tailed t-test.